

Non-contact gears: I. Next-to-leading order contribution to lateral Casimir force between corrugated parallel plates.

Inés Cavero-Peláez*

*Laboratoire Kastler Brossel, Université Pierre et Marie Curie, ENS, CNRS,
Campus Jussieu, University Paris 6, Case 74, F-75252 Paris, cedex 05, France.*

Kimball A. Milton,[†] Prachi Parashar,[‡] and K. V. Shajesh[§]

*Oklahoma Center for High Energy Physics and Homer L. Dodge Department of Physics and Astronomy,
University of Oklahoma, Norman, OK 73019, USA.*

(Dated: November 4, 2018)

We calculate the lateral Casimir force between corrugated parallel plates, described by δ -function potentials, interacting through a scalar field, using the multiple scattering formalism. The contributions to the Casimir energy due to uncorrugated parallel plates is treated as a background from the outset. We derive the leading- and next-to-leading-order contribution to the lateral Casimir force for the case when the corrugation amplitudes are small in comparison to corrugation wavelengths. We present explicit results in terms of finite integrals for the case of the Dirichlet limit, and exact results for the weak-coupling limit, for the leading- and next-to-leading-orders. The correction due to the next-to-leading contribution is significant. In the weak coupling limit we calculate the lateral Casimir force exactly in terms of a single integral which we evaluate numerically. Exact results for the case of the weak limit allows us to estimate the error in the perturbative results. We show that the error in the lateral Casimir force, in the weak coupling limit, when the next-to-leading order contribution is included is remarkably low when the corrugation amplitudes are small in comparison to corrugation wavelengths. We expect similar conclusions to hold for the Dirichlet case. The analogous calculation for the electromagnetic case should reduce the theoretical error sufficiently for comparison with the experiments.

I. INTRODUCTION

The Casimir force, as exhibited between neutral metallic parallel plates, was discovered theoretically in 1948 [1]. The Casimir torque between asymmetric materials was first studied in 1973 [2]. Recently, theoretical study of the lateral Casimir force between corrugated parallel plates was pioneered and developed by the MIT group in [3, 4, 5, 6, 7]. In particular, in [6], the authors evaluated analytic expressions for the lateral Casimir force, to the leading order, between two corrugated parallel plates perturbatively. Experimentally, the Casimir interaction between corrugated surfaces was explored during the same period of time by Roy and Mohideen in [8]. This experiment measured the lateral Casimir force between a plate, with small sinusoidal corrugations, and a large sphere with identical corrugations. The motivation was to study the nontrivial boundary dependence in the Casimir force. The experimental parameters in our notation are (see figure 1): $h = 60$ nm, $d = 1.1$ μ m, and $a = 0.1 - 0.9$ μ m, where h is the height of the corrugations, d is the wavelength of the corrugations, and a is the mean distance between the plates. The corresponding dimensionless quantities are: $k_0 a = 0.6 - 5.1$, $\frac{h}{a} = 0.07 - 0.6$, and $k_0 h = 0.3$, where k_0 is the wavenumber related to the spatial wavelength of the corrugations.

Experimental data was analyzed based on the theoretical results obtained from the proximity force approximation (PFA), and has been presented in [9, 10]. The validity of the PFA in the above analysis has been the topic of a recent debate and controversy, see [11, 12, 13]. Theoretical results based on perturbative approximations as done in [5] do not settle the issue because the error keeping only the leading order may be high. It is generally believed that the next-to-leading-order calculation will be able to throw light on the issue. We carry out this calculation for the case of scalar fields. The analogous calculation for the electromagnetic case should now be straightforward.

This paper in principle is an offshoot of [14] where we shall deal with corrugated cylinders to study non-contact gears. While evaluating the leading order for the case of corrugated cylinders it was noticed that it would be possible to extend the calculation to the next-to-leading order. This led to the study in the present paper. In this installment we

*Electronic address: cavero@spectro.jussieu.fr

[†]Electronic address: milton@nhn.ou.edu; URL: <http://www.nhn.ou.edu/%7Emilton>

[‡]Electronic address: prachi@nhn.ou.edu

[§]Electronic address: shajesh@nhn.ou.edu; URL: <http://www.nhn.ou.edu/%7Eshajesh>

present the next-to-leading-order calculation for the case of corrugated parallel plates. The leading order calculation for the corrugated cylinders, which in itself is a significant result, will form the sequel [14] of this paper. The next-to-leading-order calculation for the corrugated cylinders is in progress.

II. FORMALISM

In this section we shall describe the formalism and derive the key formula used for calculating the Casimir energy. This has been done in various papers before, (see [15], [16], [17], and references therein). We hope our derivation using Schwinger's quantum action principle techniques will be illuminating. In an earlier paper [17] describing the multiple scattering formalism it was mentioned that the use of the scattering matrix, T , was equivalent to using the full Green's function, and required the same computational effort. As a justification of this comment we exclusively use the full Green's function in this article.

A. Vacuum energy in field theory

Let us consider a scalar field, $\phi(x)$, interacting with a scalar background potential, $V(x)$, described by the Lagrangian density

$$\mathcal{L}(\phi(x)) = -\frac{1}{2} \partial_\mu \phi(x) \partial^\mu \phi(x) - \frac{1}{2} V(x) \phi(x)^2. \quad (1)$$

In terms of the source function, $K(x)$, corresponding to the scalar field, we write the action for this description to be

$$W[\phi; K] = \int d^4x \left[K(x) \phi(x) + \mathcal{L}(\phi(x)) \right]. \quad (2)$$

The vacuum to vacuum persistence amplitude,

$$Z[K] = \langle 0_+ | 0_- \rangle^K, \quad (3)$$

which generates the amplitudes for all the physical processes, satisfies Schwinger's quantum action principle,

$$\delta Z[K] = i \langle 0_+ | \delta W[\phi; K] | 0_- \rangle^K. \quad (4)$$

Our immediate task will be to get a formal solution for the vacuum amplitude, $Z[K]$, in the form

$$Z[K] = e^{iW[K]}, \quad (5)$$

where $W[K]$, which is not an action anymore, is dependent only on the source function. Note that the action, $W[\phi; K]$ in eq. (2), which satisfied the action principle, was described in terms of both the (operator) scalar field and the source function.

Variation with respect to the source function in the quantum action principle in eq. (4) allows us to write

$$\varphi(x) \equiv \frac{\langle 0_+ | \phi(x) | 0_- \rangle^K}{Z[K]} = \frac{1}{Z[K]} \frac{1}{i} \frac{\delta Z[K]}{\delta K(x)}, \quad (6)$$

where the redefined scalar field, on the left of the above expression, is an effective field. This can be used to replace operator fields with functional derivatives with respect to the sources. Variation with respect to the scalar field in eq. (4) gives us

$$-\left[\partial^2 - V(x) \right] \frac{1}{i} \frac{\delta Z[K]}{\delta K(x)} = K(x) Z[K], \quad (7)$$

which can be immediately inverted and written in the form, after using eq. (6),

$$\varphi(x) = \frac{1}{Z[K]} \frac{1}{i} \frac{\delta Z[K]}{\delta K(x)} = \int d^4x' G(x, x') K(x'), \quad (8)$$

where we defined the inverse of the differential operator, the Green's function, as

$$-\left[\partial^2 - V(x)\right] G(x, x') = \delta^{(4)}(x - x'). \quad (9)$$

The solution to eq. (8) is a Gaussian in the functional sense, and when written in the desired form in eq. (5), lets us identify

$$W[K] = Q[V] + \frac{1}{2} \int d^4x \int d^4x' K(x) G(x, x') K(x'), \quad (10)$$

where $Q[V]$ is a functional of the background potential alone. For the case when the background potential is switched off, described by $V = 0$, we have $Z_0[K] = \exp(iW_0[K])$, where

$$W_0[K] = Q[0] + \frac{1}{2} \int d^4x \int d^4x' K(x) G_0(x, x') K(x'), \quad (11)$$

where, $G_0(x, x')$ is the corresponding Green's function in eq. (9) for the case when $V = 0$. Now, in the absence of a source function the vacuum should not decay, which amounts to the statement $\langle 0_+ | 0_- \rangle^{K=0} = 1$. This implies that $W_0[0] = 0$ which when used in eq. (11) lets us conclude that $Q[0] = 0$.

Variation with respect to the background potential in eq. (4) yields

$$\delta Z[K] = -\frac{i}{2} \int d^4x \delta V(x) \langle 0_+ | \phi(x) \phi(x) | 0_- \rangle, \quad (12)$$

where we can replace the operator fields with functional derivatives and then write the formal solution as

$$Z[K] = e^{-\frac{i}{2} \int d^4x V(x) \frac{1}{\delta K(x)} \frac{\delta}{\delta K(x)}} e^{\frac{i}{2} \int d^4x \int d^4x' K(x) G_0(x, x') K(x')}. \quad (13)$$

Using the standard identity, we have

$$W[K] = -\frac{i}{2} \text{Tr} \ln G G_0^{-1} + \frac{1}{2} \int d^4x \int d^4x' K(x) G(x, x') K(x'), \quad (14)$$

which uses $(1 + G_0 V)^{-1} G_0 = G$. Using eq. (14) in eq. (5) we observe that in the presence of a background the vacuum to vacuum transition amplitude is not unity, instead it evaluates to

$$\langle 0_+ | 0_- \rangle^{K=0} = e^{iW[0]} = e^{\frac{i}{2} \text{Tr} \ln G G_0^{-1}}. \quad (15)$$

For the case when the process under investigation is time independent, denoting τ to be the time associated with the physical process, we can evolve the vacuum state using the Hamiltonian of the system and thus conclude

$$\langle 0_+ | 0_- \rangle^{K=0} = \langle 0_- | e^{-iH\tau} | 0_- \rangle = e^{-iE\tau}, \quad (16)$$

where we assumed the vacuum to be an eigenstate of the Hamiltonian. Comparing the two forms, eq. (15) and eq. (16), we thus identify the energy of the vacuum in the presence of a background to be

$$E = \frac{i}{2\tau} \text{Tr} \ln G G_0^{-1} \quad (17)$$

which serves as the central formula for calculating the Casimir energy. Further, for the case of a time independent situation, making a Fourier transformation in the time variable and using translational independence in time, we can formally write

$$E = -\frac{i}{2} \int \frac{d\omega}{2\pi} \text{Tr} \ln \left[-\omega^2 - \nabla^2 + V \right] + \frac{i}{2} \int \frac{d\omega}{2\pi} \text{Tr} \ln \left[-\omega^2 - \nabla^2 \right] \quad (18)$$

where we used eq. (9) to define the Fourier transformed Green's function in the form $\bar{G}^{-1} = [-\omega^2 - \nabla^2 + V]$. Integrating by parts and throwing away the boundary terms we derive

$$E = -\frac{i}{2} \int \frac{d\omega}{2\pi} 2\omega^2 \text{Tr} \bar{G} + \frac{i}{2} \int \frac{d\omega}{2\pi} 2\omega^2 \text{Tr} \bar{G}_0, \quad (19)$$

which is an alternate expression for evaluating the Casimir energy. This latter form has been used in studies [18] related to surface divergences which requires the evaluation of the energy density rather than the total energy.

B. Statement of the problem

We consider two semitransparent, corrugated plates, parallel to the $x - y$ plane, described by the potentials,

$$V_i(z, y) = \lambda_i \delta(z - a_i - h_i(y)), \quad (20)$$

where $i = 1, 2$, are labels that identify the individual plates, and we define $a = a_2 - a_1 > 0$. The functions $h_i(y)$ are designed to describe the corrugations associated with the individual plates. Let us define the function

$$a(y) = a + h_2(y) - h_1(y) \quad (21)$$

which measures the relative corrugations between the two plates. We shall define the corrugations $h_i(y)$ so that the mean of the relative corrugations is a . In general we require $a(y) > 0$, which is a restriction on the corrugations. Translational invariance is assumed in the x direction.

The change in energy due to the change in the mean distance between the plates, a , leads to the conventional Casimir force which points in the direction perpendicular to the surface of the plates, and is expressed as

$$F_{\text{Cas}} = -\frac{\partial E}{\partial a}, \quad (22)$$

where E is the total Casimir energy associated with the corrugated plates including the divergent contributions associated with the single plates. The divergent contributions being independent of a , do not contribute to the Casimir force. When the plates have corrugations on them we expect to have a change in the total energy due to a shift of one of the plates parallel (lateral) to the other plate. The force corresponding to the change in the total energy due to this shift acts in the lateral direction and is called the lateral Casimir force. The shift is mathematically described by a translation in the y -coordinate, $h_1(y + y_0)$, which corresponds to a lateral shift of one plate with respect to the other. The lateral force is expressed as

$$F_{\text{Lat}} = -\frac{\partial E}{\partial y_0}, \quad (23)$$

where y_0 is the measure of the translational shift.

We note that there will be no lateral force between the plates if the corrugations are switched off by setting $h_i(y) = 0$, $i = 1$ and 2 . The physical quantities associated with this configuration will thus act as a background, and a reference, and we shall find it convenient to denote them by the superscript (0) to mean zeroth order. The potential for the background will thus be described by

$$V_i^{(0)}(z) = \lambda_i \delta(z - a_i), \quad (24)$$

which has no y dependence. The total Casimir energy associated with the background, due to the two uncorrugated plates, will be denoted as $E^{(0)}$, which will include the divergent contributions associated with the single plates. This background energy will be independent of the displacement y_0 due to the y independence of this configuration. Thus, we can conclude that

$$F_{\text{Lat}}^{(0)} = -\frac{\partial E^{(0)}}{\partial y_0} = 0. \quad (25)$$

We further note that there will be no lateral force between the plates if either one of the plates have their corrugations switched off by setting $h_i(y) = 0$, $i = 1$ or 2 . The Casimir energy associated with this configuration can be written as

$$E_i = E - E^{(0)} \quad (26)$$

where E_i is the additional contribution to the energy with respect to the background energy due to the presence of the corrugations on one of the plates. Throughout this article we shall use Δ to mean the deviation from the background. For example, we will have $\Delta V_i(z, y) = V_i(z, y) - V_i^{(0)}(z)$. Using the argument of y independence, or translational symmetry, we can again conclude that

$$(F_{\text{Lat}})_i = -\frac{\partial E_i}{\partial y_0} = 0. \quad (27)$$

In light of the above observations we are led to write the total Casimir energy, for the case when both the plates have their corrugations switched on, in the form

$$\Delta E = E - E^{(0)}(a) = E_1(a, h_1) + E_2(a, h_2) + E_{12}(a, h_1, h_2, y_0), \quad (28)$$

where E_{12} is the contribution to the total energy due to the interaction between the corrugations in the plates. Only this part of the total energy contributes to the lateral Casimir force. Thus, we conclude that

$$F_{\text{Lat}} = -\frac{\partial}{\partial y_0} \Delta E = -\frac{\partial E_{12}}{\partial y_0}. \quad (29)$$

Our central problem will be to evaluate E_{12} using eq. (17).

C. Casimir energy contributing to the lateral force

Using the central formula derived in the multiple scattering formalism in eq. (17) to evaluate eq. (28) we have

$$\Delta E = E - E^{(0)} = \frac{i}{2\tau} \text{Tr} \ln GG_0^{-1} - \frac{i}{2\tau} \text{Tr} \ln G^{(0)} G_0^{-1} = \frac{i}{2\tau} \text{Tr} \ln GG^{(0)-1}, \quad (30)$$

where G_0 is the free Green's function introduced in eq. (11). Note that G_0 cancels in the above expression and the reference is now with respect to the uncorrugated plates. The Green's function G satisfies eq. (9) with potentials described by eq. (20), which in symbolic notation reads

$$\left[-\partial^2 + V_1 + V_2 \right] G = 1, \quad (31)$$

and the corresponding Green's function associated with the background satisfies the differential equation,

$$\left[-\partial^2 + V_1^{(0)} + V_2^{(0)} \right] G^{(0)} = 1. \quad (32)$$

The above two equations can be used to deduce

$$GG^{(0)-1} = \left[1 + G^{(0)} \Delta V_1 + G^{(0)} \Delta V_2 \right]^{-1}. \quad (33)$$

Next, one makes the observation that the above expression can be rewritten in the form

$$GG^{(0)-1} = G_2 G^{(0)-1} \left[1 - G_1 \Delta V_1 G_2 \Delta V_2 \right]^{-1} G_1 G^{(0)-1}, \quad (34)$$

where G_i ($i = 1, 2$) are the Green's functions for the parallel plates when only one of the plates has corrugations on it. The differential equations for G_i 's are

$$\left[-\partial^2 + V_1^{(0)} + V_2^{(0)} + \Delta V_i \right] G_i = 1, \quad (35)$$

which together with eq. (32) can be used to deduce

$$G_i G^{(0)-1} = (1 + G^{(0)} \Delta V_i)^{-1} = 1 - G^{(0)} \Delta V_i (1 + G^{(0)} \Delta V_i)^{-1} = 1 - (1 + G^{(0)} \Delta V_i)^{-1} G^{(0)} \Delta V_i. \quad (36)$$

Using eq. (34) in eq. (30) we immediately obtain eq. (28). The last term in eq. (28), E_{12} , which is the only term that contributes to the lateral force between the two corrugated plates, can be read out from eq. (34) to be given by the expression

$$E_{12} = -\frac{i}{2\tau} \text{Tr} \ln \left[1 - G_1 \Delta V_1 G_2 \Delta V_2 \right]. \quad (37)$$

We could have written this down immediately, but we hope it was instructive to go through the steps because it clarifies our notation, which would anyhow have required us to write many of the above equations, and also to emphasize that the configuration due to parallel plates is treated as a background from the outset.

D. Formal series expansion

Formally expanding the logarithm in the above expression and using eq. (36) to expand $G_i \Delta V_i$ in terms of $G^{(0)} \Delta V_i$ we can write

$$E_{12} = \frac{i}{2\tau} \text{Tr} \sum_{m=1}^{\infty} \frac{1}{m} \left[\sum_{n_1=1}^{\infty} \sum_{n_2=1}^{\infty} (-1)^{n_1} (-1)^{n_2} \left\{ G^{(0)} \Delta V_1 \right\}^{n_1} \left\{ G^{(0)} \Delta V_2 \right\}^{n_2} \right]^m. \quad (38)$$

Our potentials in eq. (20) can be formally expanded in powers of h_i in the form

$$\Delta V_i(z, y) = \sum_{n=1}^{\infty} V_i^{(n)}(z, y) = \sum_{n=1}^{\infty} \frac{[-h_i(y)]^n}{n!} \frac{\partial^n}{\partial z^n} V_i^{(0)}(z) = \lambda_i \left[e^{-h_i(y) \frac{\partial}{\partial z}} - 1 \right] \delta(z - a_i), \quad (39)$$

so we can further write the series expansion as

$$E_{12} = \frac{i}{2\tau} \text{Tr} \sum_{m=1}^{\infty} \frac{1}{m} \left[\sum_{n_1=1}^{\infty} \sum_{n_2=1}^{\infty} (-\lambda_1)^{n_1} (-\lambda_2)^{n_2} \left\{ G^{(0)} [e^{-h_1 \partial} - 1] \delta_1 \right\}^{n_1} \left\{ G^{(0)} [e^{-h_2 \partial} - 1] \delta_2 \right\}^{n_2} \right]^m, \quad (40)$$

where we again use symbolic notation and suppress the variable dependence in h_i , ∂ , and the delta functions.

III. LEADING ORDER CONTRIBUTION

In this section we shall derive the leading order contribution to the Casimir energy when the corrugation amplitude is small in comparison to the corrugation wavelength. This has been evaluated for the Dirichlet scalar case and the electromagnetic case in [5, 6]. We obtain the result for scalar δ -function potentials as a warm up exercise in preparation for the calculation for the next-to-leading order. In this section we shall illustrate our methodology which will be further used in the higher order calculation.

A. Second order perturbation in Casimir energy due to corrugations

For the particular case when the corrugations can be treated as small perturbations we can approximate the potentials by keeping a few terms in the expansion in eq. (38) where we use the superscripts (n) to represent the n -th order perturbation in a quantity. Thus, to the leading order the interaction energy of the corrugations in eq. (38) takes the form

$$E_{12}^{(2)} = \frac{i}{2\tau} \text{Tr} \left[G^{(0)} \Delta V_1^{(1)} G^{(0)} \Delta V_2^{(1)} \right]. \quad (41)$$

We observe that the potentials in the n -th order are given by derivatives acting on δ -functions in eq. (39) which can be transferred over to the Green's functions after integration by parts. The background Green's function, which is a solution to eq. (32), can be written as

$$G^{(0)}(\mathbf{x}, t, \mathbf{x}', t') = \int \frac{d\omega}{2\pi} e^{-i\omega(t-t')} \int \frac{dk_x}{2\pi} e^{ik_x(x-x')} \int \frac{dk_y}{2\pi} e^{ik_y(y-y')} g^{(0)}(z, z'; \kappa), \quad (42)$$

where $\kappa^2 = \bar{\kappa}^2 + k_y^2$, with $\bar{\kappa}^2 = k_x^2 - \omega^2$, where $k_{x,y}$ and ω are the Fourier variables corresponding to the space-time coordinates x, y and t respectively. The reduced Green's function, $g^{(0)}(z, z'; \kappa)$, satisfies the equation

$$- \left[\frac{\partial^2}{\partial z^2} - \kappa^2 - \lambda_1 \delta(z - a_1) - \lambda_2 \delta(z - a_2) \right] g^{(0)}(z, z'; \kappa) = \delta(z - z'). \quad (43)$$

In terms of the reduced Green's function defined above we can write eq. (41) as

$$\frac{E_{12}^{(2)}}{L_x} = \int_{-\infty}^{\infty} \frac{dk_1}{2\pi} \int_{-\infty}^{\infty} \frac{dk_2}{2\pi} \tilde{h}_1(k_1 - k_2) \tilde{h}_2(k_2 - k_1) L^{(2)}(k_1, k_2), \quad (44)$$

where L_x is a large length in the x direction and where $\tilde{h}_i(k)$ are the Fourier transforms of the functions $h_i(y)$, which describe the corrugations on the parallel plates,

$$\tilde{h}_i(k) = \int_{-\infty}^{\infty} dy e^{-iky} h_i(y). \quad (45)$$

The kernel $L^{(2)}(k_1, k_2)$ in eq. (44) is suitably expressed in the form

$$L^{(2)}(k_1, k_2) = -\frac{1}{4\pi} \int_0^{\infty} \bar{\kappa} d\bar{\kappa} I^{(2)}(\kappa_1, \kappa_2), \quad (46)$$

where we have switched to imaginary frequencies by a Euclidean rotation, $\omega \rightarrow i\zeta$, and defined

$$I^{(2)}(\kappa_1, \kappa_2) = \lambda_1 \lambda_2 \frac{\partial}{\partial z} \frac{\partial}{\partial \bar{z}} \left[g^{(0)}(z, \bar{z}; \kappa_1) g^{(0)}(\bar{z}, z; \kappa_2) \right] \Big|_{\bar{z}=a_1, z=a_2}, \quad (47)$$

where $\kappa_i^2 = \bar{\kappa}^2 + k_i^2$. Using the reciprocal symmetry in the Green's function in eq. (47) we deduce that

$$I^{(2)}(\kappa_1, \kappa_2) = I^{(2)}(\kappa_2, \kappa_1). \quad (48)$$

We evaluate the derivatives in the expression for $I^{(2)}(\kappa_1, \kappa_2)$, using the prescription described in appendix A, as

$$I^{(2)}(\kappa_1, \kappa_2) = -\frac{\lambda_1}{2\kappa_1} \frac{\lambda_2}{2\kappa_2} \frac{e^{-a(\kappa_1+\kappa_2)}}{\Delta_1 \Delta_2} \left[\kappa_1^2 \left(1 + \frac{\lambda_1}{2\kappa_1}\right) \left(1 + \frac{\lambda_2}{2\kappa_1}\right) + \kappa_1 \kappa_2 \left(1 + \frac{\lambda_1}{2\kappa_1}\right) \left(1 + \frac{\lambda_2}{2\kappa_2}\right) \right. \\ \left. + \kappa_1 \kappa_2 \left(1 + \frac{\lambda_1}{2\kappa_2}\right) \left(1 + \frac{\lambda_2}{2\kappa_1}\right) + \kappa_2^2 \left(1 + \frac{\lambda_1}{2\kappa_2}\right) \left(1 + \frac{\lambda_2}{2\kappa_2}\right) \right], \quad (49)$$

where Δ_i 's are given by eq. (A2) after replacing $\kappa \rightarrow \kappa_i$.

1. Dirichlet limit

For the case of the Dirichlet limit ($a\lambda_{1,2} \gg 1$) the expression for $I^{(2)}(\kappa_1, \kappa_2)$ in eq. (49) takes on the relatively simple form

$$I_D^{(2)}(\kappa_1, \kappa_2) = -\frac{\kappa_1}{\sinh \kappa_1 a} \frac{\kappa_2}{\sinh \kappa_2 a} \quad (50)$$

where the subscript D stands for Dirichlet limit. Using the above expression in eq. (46) we have

$$L_D^{(2)}(k_1, k_2) = \frac{1}{4\pi} \int_0^{\infty} \bar{\kappa} d\bar{\kappa} \frac{\kappa_1}{\sinh \kappa_1 a} \frac{\kappa_2}{\sinh \kappa_2 a}. \quad (51)$$

We describe the correspondence of the expression for the interaction energy, in eq. (44), in the Dirichlet limit, to the result in [6] in appendix B.

We shall digress a little to answer how the above result is related to the Dirichlet Green's function. We start by recalling the reduced Green's function corresponding to eq. (43) in the Dirichlet limit, which can be derived by taking the $\lambda_{1,2} \rightarrow \infty$ limit in $g_2^{(0)}(z, z'; \kappa)$ in eq. (A1b) defined in region 2 ($a_1 < z, z' < a_2$) in figure 10,

$$g_D^{(0)}(z, z'; \kappa) = \frac{\sinh \kappa(z_{<} - a_1) \sinh \kappa(a_2 - z_{>})}{\kappa \sinh \kappa a} \quad (52)$$

where $z_{<}$ and $z_{>}$ stand for $\text{Min}(z, z')$ and $\text{Max}(z, z')$ respectively. It is trivially verified that the above function satisfies the Dirichlet boundary conditions, $g_D^{(0)}(a_i, z'; \kappa) = 0$ and $g_D^{(0)}(z, a_i; \kappa) = 0$. Using eq. (52) we can evaluate

$$\left[\frac{d}{dz_{<}} \frac{d}{dz_{>}} g_D^{(0)}(z, z'; \kappa) \right]_{z_{<}=a_1, z_{>}=a_2} = -\frac{\kappa}{\sinh \kappa a}. \quad (53)$$

Using the above result eq. (50) can be expressed as the product of derivatives of two Dirichlet Green's functions. It is also worth mentioning that the result in eq. (50) can also be derived by exclusively using $g_2^{(0)}(z, z'; \kappa)$ in eq. (47) after taking the limit $\lambda_{1,2} \rightarrow \infty$. This is expected because the result in the Dirichlet limit should depend only on the quantities between the plates. Thus, all the results related to the Dirichlet limit can be derived without relying on the averaging prescription for taking derivatives described in appendix A. However, for the more general case being considered here, we require the averaging prescription to derive eq. (49).

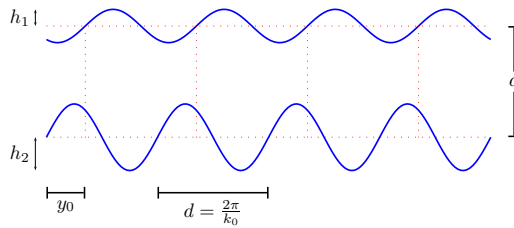


FIG. 1: Parallel plates with sinusoidal corrugations.

2. Weak coupling limit

For the weak coupling limit ($a\lambda_{1,2} \ll 1$) the expression for $I^{(2)}(\kappa_1, \kappa_2)$ in eq. (49) takes the very simple form

$$I_W^{(2)}(\kappa_1, \kappa_2) = -\frac{\lambda_1 \lambda_2}{2\kappa_1 2\kappa_2} (\kappa_1 + \kappa_2)^2 e^{-a(\kappa_1 + \kappa_2)}, \quad (54)$$

where the subscript W stands for the weak limit. We point out that in the case of weak coupling the averaging prescription for the evaluation of the I -kernels was not necessary because only the free Green's functions come in. Using the above expression in eq. (46) we can evaluate the corresponding L -kernel as

$$L_W^{(2)}(k_1, k_2) = \frac{\lambda_1 \lambda_2}{16\pi} \int_0^\infty \bar{\kappa} d\bar{\kappa} \frac{(\kappa_1 + \kappa_2)^2}{\kappa_1 \kappa_2} e^{-a(\kappa_1 + \kappa_2)} = -\frac{\lambda_1 \lambda_2}{16\pi} \frac{\partial}{\partial a} \left[\frac{1}{a} e^{-a(|k_1| + |k_2|)} \right], \quad (55)$$

where in the evaluation of the integral we used the change of variables $\kappa_1 + \kappa_2 = x$, and the corresponding relation $\bar{\kappa} d\bar{\kappa} (\kappa_1 + \kappa_2) = \kappa_1 \kappa_2 dx$.

B. Sinusoidal corrugations: Leading order

For the particular case of sinusoidal corrugations, as described in figure 1, we will have

$$h_1(y) = h_1 \sin[k_0(y + y_0)], \quad (56a)$$

$$h_2(y) = h_2 \sin[k_0 y], \quad (56b)$$

where $k_0 = 2\pi/d$ is the wavenumber corresponding to the corrugation wavelength d . We get nonzero contributions, to the leading order, only for the case when both plates have the same corrugation wavelength. The Fourier transforms $\tilde{h}_i(k)$ for sinusoidal corrugations get contributions in the form of delta functions

$$\tilde{h}_1(k) = h_1 \frac{2\pi}{2i} \left[e^{ik_0 y_0} \delta(k - k_0) - e^{-ik_0 y_0} \delta(k + k_0) \right]. \quad (57)$$

Using the above expression in eq. (44), and after interpreting $2\pi\delta(0) = L_y$ to be the infinite length in the y direction, we write

$$\frac{E_{12}^{(2)}}{L_x L_y} = \cos k_0 y_0 \frac{h_1 h_2}{4\pi} \int_{-\infty}^{\infty} dk L^{(2)}(k, k_+) = -\cos k_0 y_0 \frac{h_1 h_2}{16\pi^2} \int_{-\infty}^{\infty} dk \int_0^\infty \bar{\kappa} d\bar{\kappa} I^{(2)}(\kappa, \kappa_+), \quad (58)$$

where we have used the symmetry property in the $I^{(2)}$ -kernel, noted in eq. (48), and performed suitable rescaling in the integration variables. We have used the notations $k_\pm = k \pm k_0$, and $\kappa_\pm^2 = \bar{\kappa}^2 + k_\pm^2$. The $I^{(2)}$ -kernel in the above expression is provided by eq. (49).

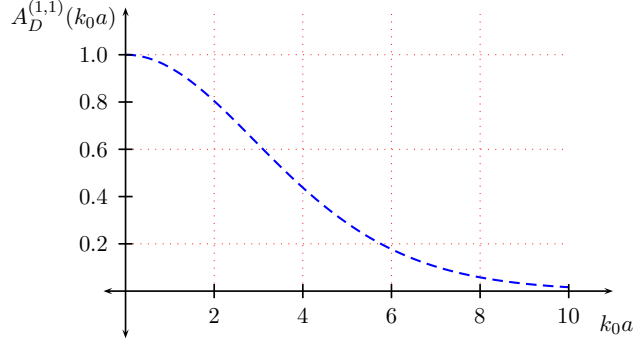


FIG. 2: Dirichlet limit: Plot of $A_D^{(1,1)}(k_0 a)$ versus $k_0 a$.

1. Dirichlet limit

In the Dirichlet limit, where the $I_D^{(2)}$ -kernel is given by eq. (50), the interaction energy in eq. (58) can be expressed in the form

$$\frac{E_{12}^{(2)}}{L_x L_y} = \cos(k_0 y_0) \frac{\pi^2}{240 a^3} \frac{h_1}{a} \frac{h_2}{a} A_D^{(1,1)}(k_0 a), \quad (59)$$

where the function $A_D^{(1,1)}(k_0 a)$ is normalized such that $A_D^{(1,1)}(0) = 1$, which becomes a convenience when we compare the results with those obtained by the proximity force approximation. The expression for $A_D^{(1,1)}(k_0 a)$ is

$$A_D^{(1,1)}(k_0 a) = \frac{60 a^5}{\pi^3} \int_{-\infty}^{\infty} dk L_D^{(2)}(k, k_+) = -\frac{1}{4\pi} \frac{60 a^5}{\pi^3} \int_{-\infty}^{\infty} dk \int_0^{\infty} \bar{\kappa} d\bar{\kappa} I_D^{(2)}(\kappa, \kappa_+), \quad (60)$$

where the $I_D^{(2)}$ -kernel, and the corresponding $L_D^{(2)}$ -kernel, in the Dirichlet limit were given in eq. (50) and eq. (51) respectively. Using the notations, $s^2 = \bar{s}^2 + t^2$, $s_{\pm}^2 = \bar{s}^2 + (t \pm t_0)^2$, and $t_0 = k_0 a$, we can write

$$A_D^{(1,1)}(t_0) = \frac{15}{\pi^4} \int_0^{\infty} \bar{s} d\bar{s} \int_{-\infty}^{\infty} dt \frac{s}{\sinh s} \frac{s_+}{\sinh s_+}. \quad (61)$$

This expression can be numerically evaluated and has been plotted in figure 2. The value of the function at $t_0 = 0$ can be evaluated exactly by rewriting the integral in terms of spherical polar coordinates to yield

$$A_D^{(1,1)}(0) = \frac{30}{\pi^4} \int_0^{\infty} s^2 ds \left[\frac{s}{\sinh s} \right]^2 = 1. \quad (62)$$

It should be mentioned that the result corresponding to eq. (61) for the electromagnetic case and the scalar Dirichlet case have been evaluated exactly in [6].

The lateral Casimir force can be evaluated using eq. (59) in the definition of lateral force in eq. (29) which yields

$$F_{\text{Lat,D}}^{(2)} = 2 k_0 a \sin(k_0 y_0) \left| F_{\text{Cas,D}}^{(0)} \right| \frac{h_1}{a} \frac{h_2}{a} A_D^{(1,1)}(k_0 a), \quad (63)$$

where $|F_{\text{Cas,D}}^{(0)}|$ is the magnitude of the normal scalar Casimir force between two uncorrugated parallel Dirichlet plates given as

$$\frac{F_{\text{Cas,D}}^{(0)}}{L_x L_y} = -\frac{\pi^2}{480} \frac{1}{a^4}. \quad (64)$$

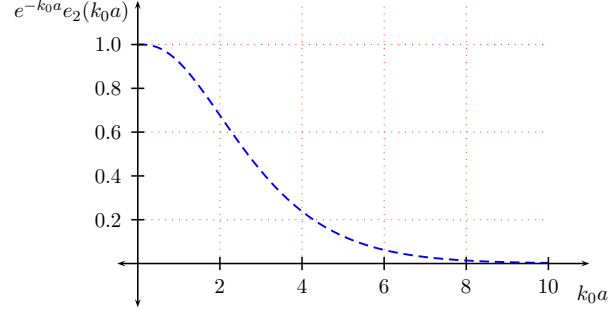


FIG. 3: Weak coupling limit: Plot of $A_W^{(2)}(k_0 a) = e^{-k_0 a} e_2(k_0 a)$ versus $k_0 a$.

2. Weak coupling limit

Let us start by recalling the expression for the Casimir energy and Casimir force between uncorrugated parallel plates in the weak limit:

$$\frac{E_{\text{Cas,W}}^{(0)}}{L_x L_y} = -\frac{\lambda_1 \lambda_2}{32 \pi^2} \frac{1}{a} \quad \text{and} \quad \frac{F_{\text{Cas,W}}^{(0)}}{L_x L_y} = -\frac{\lambda_1 \lambda_2}{32 \pi^2} \frac{1}{a^2}. \quad (65)$$

In the weak limit we have seen that it is possible to evaluate the L -kernel in eq. (55) without any effort. Using this in eq. (58) we have

$$\frac{E_{12,W}^{(2)}}{L_x L_y} = -\cos(k_0 y_0) \frac{\lambda_1 \lambda_2}{16 \pi} \frac{h_1 h_2}{4 \pi} \frac{\partial}{\partial a} \left[\frac{1}{a} \int_{-\infty}^{\infty} dk e^{-a(|k|+|k+k_0|)} \right], \quad (66)$$

which after performing the integral can be written in the form

$$E_{12,W}^{(2)} = \cos(k_0 y_0) \left| E_{\text{Cas,W}}^{(0)} \right| \frac{h_1}{a} \frac{h_2}{a} A_W^{(2)}(k_0 a), \quad (67)$$

where we have introduced the function

$$A_W^{(2)}(t_0) = \frac{t_0^3}{2} \frac{\partial^2}{\partial t_0^2} \left[\frac{1}{t_0} e^{-t_0} \right] = e^{-t_0} \sum_{m=0}^2 \frac{t_0^m}{m!} = \frac{e_2(t_0)}{e^{t_0}}, \quad (68)$$

where $e_n(x) = \sum_{m=0}^n \frac{x^m}{m!}$ is the truncated exponential function which approximates to unity for $x \ll n$. $A_W^{(2)}(t_0)$ has been plotted in figure 3. Using eq. (29) we evaluate the lateral Casimir force in this perturbation order as

$$F_{\text{Lat,W}}^{(2)} = k_0 a \sin(k_0 y_0) \left| F_{\text{Cas,W}}^{(0)} \right| \frac{h_1}{a} \frac{h_2}{a} A_W^{(2)}(k_0 a). \quad (69)$$

IV. NEXT-TO-LEADING ORDER CONTRIBUTION

We start by collecting the terms in eq. (38) in the form

$$E_{12} = E_{12}^{(2)} + E_{12}^{(3)} + E_{12}^{(4)} + \mathcal{O}(h/a)^5. \quad (70)$$

To economize typographical space and for bookkeeping purposes we introduce the notation

$$[G^{(0)} \Delta V]_{(i_1, i_2, \dots, i_N)}^{(m_1, m_2, \dots, m_N)} = \text{Tr} \left[G^{(0)} \Delta V_{i_1}^{(m_1)} G^{(0)} \Delta V_{i_2}^{(m_2)} \dots G^{(0)} \Delta V_{i_N}^{(m_N)} \right], \quad (71)$$

where the superscripts m_n denote the m_n -th order contribution in the power series expansion of the potential as defined in eq. (39). The subscript i_n identifies the potential that is contributing. In the case under consideration we have only two potentials coupling and thus $i_n = 1, 2$ for any n . As an illustrative example we have

$$[G^{(0)}\Delta V]_{(1,1,2)}^{(2,1,1)} = \text{Tr} \left[G^{(0)}\Delta V_1^{(2)} G^{(0)}\Delta V_1^{(1)} G^{(0)}\Delta V_2^{(1)} \right]. \quad (72)$$

Using the above notation we can write

$$E_{12}^{(3)} = \frac{i}{2\tau} \left\{ [G^{(0)}\Delta V]_{(1,2)}^{(2,1)} + [G^{(0)}\Delta V]_{(1,2)}^{(1,2)} - [G^{(0)}\Delta V]_{(1,1,2)}^{(1,1,1)} - [G^{(0)}\Delta V]_{(1,2,2)}^{(1,1,1)} \right\}. \quad (73)$$

We argue that for the case of sinusoidal corrugations of the same wavelength on both plates the third order perturbation does not contribute. (Contributions from third order are nonzero if the wavelength of the corrugations of one plate is double that of the other plate.) Since the plates under consideration are infinite in extent, the interaction energy is independent of translations in the y direction. Let us now make a translation of the amount $k_0 y = \pi$ in the potentials in eq. (56). This amounts to replacing $h_i \rightarrow -h_i$. Thus invariance under translation requires that the total power of h_i 's in the result should be even. This rules out the third order perturbation from contributing.

A. Fourth order perturbation in Casimir energy due to corrugations

Starting from eq. (38) and keeping terms contributing to the fourth order we have

$$E_{12}^{(4)} = E_{12}^{(2,2)} + E_{12}^{(3,1)} + E_{12}^{(1,3)}, \quad (74)$$

where the superscripts represent the powers of h_i 's. For example, the superscript (3, 1) represents terms involving $h_1^3 h_2$. All terms except one gets contribution from $m = 1$ in the logarithm expansion in eq. (38). Since the $m = 2$ term is distinct in structure we further separate it out by defining

$$E_{12}^{(2,2)} = E_{12}^{(2,2)A} + E_{12}^{(2,2)B}, \quad (75)$$

where the term involving the superscript A is the contribution from $m = 2$ in (38). Using the notation in eq. (71) we can thus collect the terms contributing to eq. (74) and eq. (75) as

$$E_{12}^{(2,2)A} = \frac{i}{2\tau} \left\{ \frac{1}{2} [G^{(0)}\Delta V]_{(1,2,1,2)}^{(1,1,1,1)} \right\}, \quad (76a)$$

$$E_{12}^{(2,2)B} = \frac{i}{2\tau} \left\{ [G^{(0)}\Delta V]_{(1,1,2,2)}^{(1,1,1,1)} - [G^{(0)}\Delta V]_{(1,1,2)}^{(1,1,2)} - [G^{(0)}\Delta V]_{(1,2,2)}^{(2,1,1)} + [G^{(0)}\Delta V]_{(1,2)}^{(2,2)} \right\}, \quad (76b)$$

$$E_{12}^{(3,1)} = \frac{i}{2\tau} \left\{ [G^{(0)}\Delta V]_{(1,1,1,2)}^{(1,1,1,1)} - [G^{(0)}\Delta V]_{(1,1,2)}^{(1,2,1)} - [G^{(0)}\Delta V]_{(1,1,2)}^{(2,1,1)} + [G^{(0)}\Delta V]_{(1,2)}^{(3,1)} \right\}, \quad (76c)$$

$$E_{12}^{(1,3)} = \frac{i}{2\tau} \left\{ [G^{(0)}\Delta V]_{(1,2,2,2)}^{(1,1,1,1)} - [G^{(0)}\Delta V]_{(1,2,2)}^{(1,2,1)} - [G^{(0)}\Delta V]_{(1,2,2)}^{(1,1,2)} + [G^{(0)}\Delta V]_{(1,2)}^{(1,3)} \right\}. \quad (76d)$$

In terms of the reduced Green's function defined in eq. (42) and eq. (43), and the Fourier transform of the corrugations in eq. (45), we can write each of the terms in eq. (76) in terms of a corresponding L -kernel. In terms of the notation introduced in eq. (71) these will read as

$$(-1)^N \frac{i}{2\tau} [G^{(0)}\Delta V]_{(i_1, \dots, i_N)}^{(m_1, \dots, m_N)} = L_x \int \frac{dk_1}{2\pi} \dots \frac{dk_N}{2\pi} \tilde{h}_{i_1}^{m_1}(k_1 - k_2) \dots \tilde{h}_{i_N}^{m_N}(k_N - k_1) L_{(i_1, \dots, i_N)}^{(m_1, \dots, m_N)}(k_1, \dots, k_N), \quad (77)$$

where implicitly we have interpreted the powers of the Fourier transformed corrugations as

$$\tilde{h}_{i_1}^{m_1}(k_1 - k_2) = \int \frac{dq_1}{2\pi} \dots \frac{dq_{m_1-1}}{2\pi} \tilde{h}_{i_1}(k_1 - q_1) \tilde{h}_{i_1}(q_1 - q_2) \dots \tilde{h}_{i_1}(q_{m_1-1} - k_2). \quad (78)$$

Observe that each term contributing to the M -th order ($M = m_1 + m_2 + \dots + m_N$) has exactly M h 's. Also, the total number of variables inside the L -kernel is N which is in general less than or equal to M . It might be appropriate to call them N -point kernels. Proceeding further, in the spirit of the second order calculation in eq. (46), we introduce the corresponding I -kernels for the L -kernels as

$$L_{(i_1, \dots, i_N)}^{(m_1, \dots, m_N)}(k_1, \dots, k_N) = -\frac{1}{4\pi} \int_0^\infty \bar{\kappa} d\bar{\kappa} I_{(i_1, \dots, i_N)}^{(m_1, \dots, m_N)}(\kappa_1, \dots, \kappa_N), \quad (79)$$

where the I -kernels are expressed in terms of derivatives operating on the reduced Green's function defined in eq. (43) as

$$I_{(i_1, \dots, i_N)}^{(m_1, \dots, m_N)}(\kappa_1, \dots, \kappa_N) = (-1)^N \frac{\lambda_{i_1}}{m_1!} \dots \frac{\lambda_{i_N}}{m_N!} \frac{\partial^{m_1}}{\partial z_1^{m_1}} \dots \frac{\partial^{m_N}}{\partial z_N^{m_N}} \left[g^{(0)}(z_N, z_1; \kappa_1) \dots g^{(0)}(z_{N-1}, z_N; \kappa_N) \right] \Big|_{z_n = a_{i_n}}. \quad (80)$$

For clarification we illustrate the evaluation of a particular term which should also serve as an illustration of the notation. The term we consider is

$$\begin{aligned} -\frac{i}{2\pi} [G^{(0)} \Delta V]_{(1,1,2)}^{(1,2,1)} &= L_x \int \frac{dk_1}{2\pi} \frac{dk_2}{2\pi} \frac{dk_3}{2\pi} \tilde{h}_1(k_1 - k_2) \tilde{h}_1^2(k_2 - k_3) \tilde{h}_2(k_3 - k_1) L_{(1,1,2)}^{(1,2,1)}(k_1, k_2, k_3) \\ &= L_x \int \frac{dk_1}{2\pi} \frac{dk_2}{2\pi} \frac{dk_3}{2\pi} \frac{dk_4}{2\pi} \tilde{h}_1(k_1 - k_2) \tilde{h}_1(k_2 - k_3) \tilde{h}_1(k_3 - k_4) \tilde{h}_2(k_4 - k_1) L_{(1,1,2)}^{(1,2,1)}(k_1, k_2, k_4). \end{aligned} \quad (81)$$

Notice how the particular k dependence in the L -kernel is unambiguously specified. The corresponding I -kernel using eq. (79) and eq. (80) is given as

$$I_{(1,1,2)}^{(1,2,1)}(\kappa_1, \kappa_2, \kappa_4) = -\frac{\lambda_1^2 \lambda_2}{2} \frac{\partial}{\partial z_1} \frac{\partial^2}{\partial z_2^2} \frac{\partial}{\partial z_3} \left[g^{(0)}(z_3, z_1; \kappa_1) g^{(0)}(z_1, z_2; \kappa_2) g^{(0)}(z_2, z_3; \kappa_4) \right] \Big|_{z_1 = a_1, z_2 = a_1, z_3 = a_2}. \quad (82)$$

Using the reciprocal symmetry in the Green's functions we can learn the following symmetries in the I -kernels associated with the terms in eq. (76):

$$I_{(1,2,1,2)}^{(1,1,1,1)}(\kappa_1, \kappa_2, \kappa_3, \kappa_4) = I_{(1,2,1,2)}^{(1,1,1,1)}(\kappa_2, \kappa_1, \kappa_4, \kappa_3), \quad I_{(1,1,2)}^{(1,1,2)}(\kappa_1, \kappa_2, \kappa_3) = I_{(1,1,2)}^{(1,1,2)}(\kappa_3, \kappa_2, \kappa_1), \quad (83a)$$

$$I_{(1,1,2,2)}^{(1,1,1,1)}(\kappa_1, \kappa_2, \kappa_3, \kappa_4) = I_{(1,1,2,2)}^{(1,1,1,1)}(\kappa_3, \kappa_2, \kappa_1, \kappa_4), \quad I_{(1,2,2)}^{(2,1,1)}(\kappa_1, \kappa_2, \kappa_3) = I_{(1,2,2)}^{(2,1,1)}(\kappa_2, \kappa_1, \kappa_3), \quad (83b)$$

$$I_{(1,2,2,2)}^{(1,1,1,1)}(\kappa_1, \kappa_2, \kappa_3, \kappa_4) = I_{(1,2,2,2)}^{(1,1,1,1)}(\kappa_2, \kappa_1, \kappa_4, \kappa_3), \quad I_{(1,2,2)}^{(1,2,1)}(\kappa_1, \kappa_2, \kappa_3) = I_{(1,2,2)}^{(1,2,1)}(\kappa_2, \kappa_1, \kappa_3), \quad (83c)$$

$$I_{(1,1,1,2)}^{(1,1,1,1)}(\kappa_1, \kappa_2, \kappa_3, \kappa_4) = I_{(1,1,1,2)}^{(1,1,1,1)}(\kappa_4, \kappa_3, \kappa_2, \kappa_1), \quad I_{(1,1,2)}^{(1,2,1)}(\kappa_1, \kappa_2, \kappa_3) = I_{(1,1,2)}^{(1,2,1)}(\kappa_3, \kappa_2, \kappa_1). \quad (83d)$$

We have not listed the 2-point I -kernels in the above list because they have the symmetry of the kind in eq. (48). In fact any 2-point kernel will have the following symmetry:

$$I_{(1,2)}^{(m_1, m_2)}(\kappa_1, \kappa_2) = I_{(1,2)}^{(m_1, m_2)}(\kappa_2, \kappa_1). \quad (84)$$

In the above discussion involving very general notations we have in principle expressed each term in eq. (76). Specific evaluation of each term involves the evaluation of the corresponding I -kernels which are given in terms of the derivatives of the Green's functions. The derivatives are evaluated using the prescription described in appendix A. We can thus collect the terms in eq. (76) into four distinct L -kernels in the form

$$\frac{E_{12}^{(2,2)A}}{L_x} = \frac{1}{2} \int \frac{dk_1}{2\pi} \frac{dk_2}{2\pi} \frac{dk_3}{2\pi} \frac{dk_4}{2\pi} \tilde{h}_1(k_1 - k_2) \tilde{h}_2(k_2 - k_3) \tilde{h}_1(k_3 - k_4) \tilde{h}_2(k_4 - k_1) L^{(2,2)A}(k_1, k_2, k_3, k_4), \quad (85a)$$

$$\frac{E_{12}^{(2,2)B}}{L_x} = \int \frac{dk_1}{2\pi} \frac{dk_2}{2\pi} \frac{dk_3}{2\pi} \frac{dk_4}{2\pi} \tilde{h}_1(k_1 - k_2) \tilde{h}_1(k_2 - k_3) \tilde{h}_2(k_3 - k_4) \tilde{h}_2(k_4 - k_1) L^{(2,2)B}(k_1, k_2, k_3, k_4), \quad (85b)$$

$$\frac{E_{12}^{(3,1)}}{L_x} = \int \frac{dk_1}{2\pi} \frac{dk_2}{2\pi} \frac{dk_3}{2\pi} \frac{dk_4}{2\pi} \tilde{h}_1(k_1 - k_2) \tilde{h}_1(k_2 - k_3) \tilde{h}_1(k_3 - k_4) \tilde{h}_2(k_4 - k_1) L^{(3,1)}(k_1, k_2, k_3, k_4), \quad (85c)$$

$$\frac{E_{12}^{(1,3)}}{L_x} = \int \frac{dk_1}{2\pi} \frac{dk_2}{2\pi} \frac{dk_3}{2\pi} \frac{dk_4}{2\pi} \tilde{h}_1(k_1 - k_2) \tilde{h}_2(k_2 - k_3) \tilde{h}_2(k_3 - k_4) \tilde{h}_2(k_4 - k_1) L^{(1,3)}(k_1, k_2, k_3, k_4), \quad (85d)$$

where it should be noted that different L 's combine with specific combination of h 's. The factor of one-half in eq. (85a) can be traced back to the coefficient of the second term in the expansion of logarithm in eq. (38). The respective kernels $L^{(m,n)}$ above are related to their corresponding $I^{(m,n)}$ by eq. (79), which are given by

$$I^{(2,2)A}(\kappa_1, \kappa_2, \kappa_3, \kappa_4) = I_{(1,2,1,2)}^{(1,1,1,1)}(\kappa_1, \kappa_2, \kappa_3, \kappa_4), \quad (86a)$$

$$I^{(2,2)B}(\kappa_1, \kappa_2, \kappa_3, \kappa_4) = I_{(1,1,2,2)}^{(1,1,1,1)}(\kappa_1, \kappa_2, \kappa_3, \kappa_4) + I_{(1,1,2)}^{(1,1,2)}(\kappa_1, \kappa_2, \kappa_3) + I_{(1,2,2)}^{(2,1,1)}(\kappa_1, \kappa_3, \kappa_4) + I_{(1,2)}^{(2,2)}(\kappa_1, \kappa_3), \quad (86b)$$

$$I^{(3,1)}(\kappa_1, \kappa_2, \kappa_3, \kappa_4) = I_{(1,1,1,2)}^{(1,1,1,1)}(\kappa_1, \kappa_2, \kappa_3, \kappa_4) + I_{(1,1,2)}^{(1,2,1)}(\kappa_1, \kappa_2, \kappa_4) + I_{(1,1,2)}^{(2,1,1)}(\kappa_1, \kappa_3, \kappa_4) + I_{(1,2)}^{(3,1)}(\kappa_1, \kappa_4), \quad (86c)$$

$$I^{(1,3)}(\kappa_1, \kappa_2, \kappa_3, \kappa_4) = I_{(1,2,2,2)}^{(1,1,1,1)}(\kappa_1, \kappa_2, \kappa_3, \kappa_4) + I_{(1,2,2)}^{(1,2,1)}(\kappa_1, \kappa_2, \kappa_4) + I_{(1,2,2)}^{(1,1,2)}(\kappa_1, \kappa_2, \kappa_3) + I_{(1,2)}^{(1,3)}(\kappa_1, \kappa_2). \quad (86d)$$

Proceeding in the spirit of section III has brought us to the point of evaluation of the thirteen I -kernels on the right hand side of eq. (86). Using the prescription described in appendix A we have evaluated all the thirteen kernels and explicit expressions analogous to eq. (49) have been derived. This would have involved a lot more labor and bookkeeping if not for the facilitation achieved by the use of Mathematica. We shall not display the explicit expressions here because they are too long. But, as in section III, these expressions simplify considerably in the Dirichlet limit and the weak coupling limit.

1. Dirichlet limit

Observe that the reduced Green's function defined by eq. (43) has a well defined Dirichlet limit. In the light of this observation in conjunction with the expression for the I -kernels in eq. (80) taken at face value suggests that these kernels might not have a well-defined finite Dirichlet limit. However, we evaluated the second order contribution in eq. (50). In fact it can be verified that all 2-point kernels have a well-defined finite Dirichlet limit. Further, $I_{(1,2,1,2)}^{(1,1,1,1)}$ also has a well-defined finite Dirichlet limit. The rest of the nine I -kernels on the right hand side of eq. (86) do not have a finite Dirichlet limit. But, the sums of the I -kernels listed in eq. (86) have finite Dirichlet limits. The higher powers in $\lambda_{1,2}$ in the numerator of each of these sums cancel identically to give a well-defined limit as $\lambda_{1,2} \rightarrow \infty$. This seems to be a generic phenomena. Here we list the I -kernels in eq. (86) evaluated in the Dirichlet limit:

$$I_D^{(2,2)A}(\kappa_1, \kappa_2, \kappa_3, \kappa_4) = \frac{\kappa_1}{\sinh \kappa_1 a} \frac{\kappa_2}{\sinh \kappa_2 a} \frac{\kappa_3}{\sinh \kappa_3 a} \frac{\kappa_4}{\sinh \kappa_4 a}, \quad (87a)$$

$$I_D^{(2,2)B}(\kappa_1, \kappa_2, \kappa_3, \kappa_4) = \frac{\kappa_1}{\sinh \kappa_1 a} \frac{\kappa_2}{\tanh \kappa_2 a} \frac{\kappa_3}{\sinh \kappa_3 a} \frac{\kappa_4}{\tanh \kappa_4 a}, \quad (87b)$$

$$I_D^{(3,1)}(\kappa_1, \kappa_2, \kappa_3, \kappa_4) = -\frac{\kappa_1}{\sinh \kappa_1 a} \frac{\kappa_4}{\sinh \kappa_4 a} \frac{1}{4} \left[4 \frac{\kappa_2}{\tanh \kappa_2 a} \frac{\kappa_3}{\tanh \kappa_3 a} + \frac{\kappa_1^2 + \kappa_4^2}{3} - \kappa_2^2 - \kappa_3^2 \right], \quad (87c)$$

$$I_D^{(1,3)}(\kappa_1, \kappa_2, \kappa_3, \kappa_4) = -\frac{\kappa_1}{\sinh \kappa_1 a} \frac{\kappa_2}{\sinh \kappa_2 a} \frac{1}{4} \left[4 \frac{\kappa_3}{\tanh \kappa_3 a} \frac{\kappa_4}{\tanh \kappa_4 a} + \frac{\kappa_1^2 + \kappa_2^2}{3} - \kappa_3^2 - \kappa_4^2 \right]. \quad (87d)$$

2. Weak coupling limit

We can similarly evaluate the I -kernels in the weak limit by keeping terms to order $\lambda_1 \lambda_2$ in the general expressions for the I -kernels. But, we find it instructive, and simpler, to start over from eq. (76). We observe that only the 2-point kernels contribute in the weak limit. We further notice that only the contributions from the free Green's function (which is obtained by switching off the couplings $\lambda_{1,2}$ in eq. (43)) contribute in the evaluation of the weak limit. These observations allows us to write the 2-point kernels in the weak limit as

$$\begin{aligned} I_{(1,2),W}^{(m_1,m_2)}(\kappa_1, \kappa_2) &= \frac{\lambda_1}{m_1!} \frac{\lambda_2}{m_2!} \left[\frac{\partial^{m_1}}{\partial z_1^{m_1}} \frac{\partial^{m_2}}{\partial z_2^{m_2}} \frac{e^{-\kappa_1|z_2-z_1|}}{2\kappa_1} \frac{e^{-\kappa_2|z_1-z_2|}}{2\kappa_2} \right]_{z_1=a_1, z_2=a_2} \\ &= \frac{(-1)^{m_1}}{m_1! m_2!} \frac{\lambda_1 \lambda_2}{2\kappa_1 2\kappa_2} (\kappa_1 + \kappa_2)^M e^{-a(\kappa_1 + \kappa_2)}, \end{aligned} \quad (88)$$

where $M = m_1 + m_2$. Note that the derivatives in the above expressions are well defined because they are evaluated at a point where $z_2 > z_1$. In particular using these in eq. (86) with the observation that only the 2-point kernels contribute in the weak limit we get $I_W^{(2,2)A}(\kappa_1, \kappa_2, \kappa_3, \kappa_4) = 0$ and

$$I_W^{(2,2)B}(\kappa_1, \kappa_2, \kappa_3, \kappa_4) = I_{(1,2),W}^{(2,2)}(\kappa_1, \kappa_3) = \frac{1}{2! 2!} \frac{\lambda_1 \lambda_2}{2\kappa_1 2\kappa_3} (\kappa_1 + \kappa_3)^4 e^{-a(\kappa_1 + \kappa_3)}, \quad (89a)$$

$$I_W^{(3,1)}(\kappa_1, \kappa_2, \kappa_3, \kappa_4) = I_{(1,2),W}^{(3,1)}(\kappa_1, \kappa_4) = \frac{1}{3! 1!} \frac{\lambda_1 \lambda_2}{2\kappa_1 2\kappa_4} (\kappa_1 + \kappa_4)^4 e^{-a(\kappa_1 + \kappa_4)}, \quad (89b)$$

$$I_W^{(1,3)}(\kappa_1, \kappa_2, \kappa_3, \kappa_4) = I_{(1,2),W}^{(1,3)}(\kappa_1, \kappa_2) = \frac{1}{1! 3!} \frac{\lambda_1 \lambda_2}{2\kappa_1 2\kappa_2} (\kappa_1 + \kappa_2)^4 e^{-a(\kappa_1 + \kappa_2)}, \quad (89c)$$

where notice how they differ in the particular dependence on the variables. We again (see comments after eq. (54)) point out that the averaging prescription for the evaluation of the I -kernels was not necessary to arrive at the above expressions.

Using the change of variables introduced in evaluating eq. (55) we can similarly evaluate the L -kernels using eq. (79) in the weak limit as

$$L_{(1,2),W}^{(m_1,m_2)}(k_1, k_2) = \frac{(-1)^{m_2}}{m_1! m_2!} \frac{\lambda_1 \lambda_2}{16 \pi} \left(\frac{\partial}{\partial a} \right)^{M-1} \left[\frac{1}{a} e^{-a(|k_1|+|k_2|)} \right], \quad (90)$$

which reproduces the result in eq. (55) for $M = 2$.

B. Sinusoidal corrugations: Next-to-leading order

We shall now specialize to the particular case of sinusoidal corrugations described by eq. (56). Using the Fourier transforms in eq. (57) all but one of the k integrals in eq. (85) can be immediately performed. The symmetries listed in eq. (83) lead to simplifications in the expressions. As in section III the expressions boil down to two integrals in variables k and $\bar{\kappa}$. In particular eq. (85) takes the form

$$\frac{E_{12}^{(2,2)}}{L_x L_y} = -\cos(2k_0 y_0) \frac{h_1^2 h_2^2}{64 \pi^2} \int_{-\infty}^{\infty} dk \int_0^{\infty} \bar{\kappa} d\bar{\kappa} \left[\frac{1}{2} I^{(2,2)A}(\kappa, \kappa_+, \kappa, \kappa_+) + I^{(2,2)B}(\kappa_-, \kappa, \kappa_+, \kappa) \right], \quad (91a)$$

$$\frac{E_{12}^{(3,1)}}{L_x L_y} = -\cos(k_0 y_0) \frac{h_1^3 h_2}{64 \pi^2} \int_{-\infty}^{\infty} dk \int_0^{\infty} \bar{\kappa} d\bar{\kappa} \left[I^{(3,1)}(\kappa, \kappa_+, \kappa, \kappa_+) + I^{(3,1)}(\kappa, \kappa_+, \kappa, \kappa_-) + I^{(3,1)}(\kappa, \kappa_-, \kappa, \kappa_+) \right], \quad (91b)$$

$$\frac{E_{12}^{(1,3)}}{L_x L_y} = -\cos(k_0 y_0) \frac{h_1 h_2^3}{64 \pi^2} \int_{-\infty}^{\infty} dk \int_0^{\infty} \bar{\kappa} d\bar{\kappa} \left[I^{(1,3)}(\kappa, \kappa_+, \kappa, \kappa_+) + I^{(1,3)}(\kappa, \kappa_+, \kappa, \kappa_-) + I^{(1,3)}(\kappa, \kappa_-, \kappa, \kappa_+) \right], \quad (91c)$$

where the I -kernels are given from eq. (86). We use the notations k_{\pm} and κ_{\pm} introduced after eq. (58). We note the factor of 2 in the argument of cosine function of the first term above is a mark of the fourth order in perturbation theory. It should be mentioned here that in the above expressions we have omitted finite terms not having any dependence in the lateral shift variable y_0 . These terms do not contribute to the lateral force.

1. Dirichlet limit

We presented the expressions for the I -kernels in the Dirichlet limit in eq. (87). Using these in eq. (91) and then adding the contributions from the three terms in eq. (74) we can write the total contribution to interaction energy due to the presence of corrugations as

$$\frac{E_{12}^{(4)}}{L_x L_y} = \frac{\pi^2}{240} \frac{h_1}{a^3} \frac{h_2}{a} \frac{15}{4} \left[\cos(k_0 y_0) \left\{ \frac{h_1^2}{a^2} A_D^{(3,1)}(k_0 a) + \frac{h_2^2}{a^2} A_D^{(1,3)}(k_0 a) \right\} - \cos(2k_0 y_0) \frac{1}{2} \frac{h_1}{a} \frac{h_2}{a} A_D^{(2,2)}(k_0 a) \right], \quad (92)$$

where we have introduced the functions

$$A_D^{(3,1)}(t_0) = A_D^{(1,3)}(t_0) = \frac{1}{2\pi^4} \int_0^{\infty} \bar{s} d\bar{s} \int_{-\infty}^{\infty} dt \frac{s}{\sinh s} \frac{s_+}{\sinh s_+} \left[4 \frac{s}{\tanh s} \frac{s_-}{\tanh s_-} + 2 \frac{s}{\tanh s} \frac{s_+}{\tanh s_+} - s^2 - s_-^2 \right], \quad (93a)$$

$$A_D^{(2,2)}(t_0) = \frac{1}{\pi^4} \int_0^{\infty} \bar{s} d\bar{s} \int_{-\infty}^{\infty} dt \left[\frac{s^2}{\sinh^2 s} \frac{s_-^2}{\sinh^2 s_-} + 2 \frac{s^2}{\tanh^2 s} \frac{s_+}{\sinh s_+} \frac{s_-}{\sinh s_-} \right]. \quad (93b)$$

These functions are plotted in figure 4. As in section III the above functions are suitably normalized such that they evaluate to unity when evaluated at $t_0 = 0$. Verification of this statement involves the following integrals:

$$A_D^{(3,1)}(0) = \frac{2}{\pi^4} \int_0^{\infty} s^2 ds \frac{s^2}{\sinh^2 s} \left[3 \frac{s^2}{\tanh^2 s} - s^2 \right] = \left(1 + \frac{\pi^2}{21} \right) - \frac{\pi^2}{21} = 1, \quad (94a)$$

$$A_D^{(2,2)}(0) = \frac{2}{\pi^4} \int_0^{\infty} s^2 ds \left[\frac{s^4}{\sinh^4 s} + 2 \frac{s^2}{\tanh^2 s} \frac{s^2}{\sinh^2 s} \right] = \left(\frac{1}{3} + \frac{2\pi^2}{63} \right) + \left(\frac{2}{3} - \frac{2\pi^2}{63} \right) = 1. \quad (94b)$$

Therefore, the next-to-leading-order contribution to the lateral Casimir force in the Dirichlet limit reads

$$F_{\text{Lat,D}}^{(4)} = 2 k_0 a \sin(k_0 y_0) \left| F_{\text{Cas,D}}^{(0)} \right| \frac{h_1}{a} \frac{h_2}{a} \frac{15}{4} \left[\left(\frac{h_1^2}{a^2} + \frac{h_2^2}{a^2} \right) A_D^{(3,1)}(k_0 a) - 2 \cos(k_0 y_0) \frac{h_1}{a} \frac{h_2}{a} A_D^{(2,2)}(k_0 a) \right]. \quad (95)$$

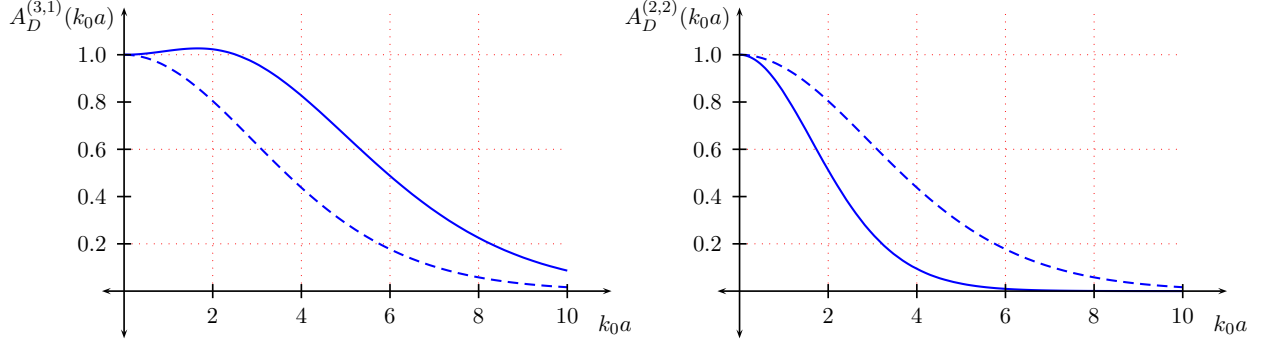


FIG. 4: Dirichlet limit: Plot of $A_D^{(3,1)}(k_0 a)$ and $A_D^{(2,2)}(k_0 a)$ versus $k_0 a$. The dashed curve represents $A_D^{(1,1)}(k_0 a)$ which is plotted here for reference.

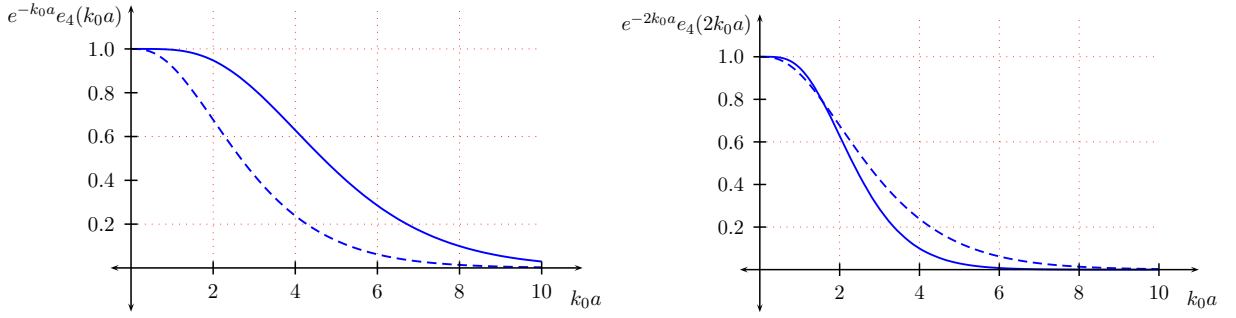


FIG. 5: Weak coupling limit: Plot of $A_W^{(4)}(k_0 a)$ and $A_W^{(4)}(2k_0 a)$ versus $k_0 a$. The dashed curve represents $A_W^{(2)}(k_0 a)$ which is plotted here for reference.

2. Weak coupling limit

We have already evaluated the L -kernel for the weak coupling case in eq (90), so we can immediately evaluate the interaction energy. Alternatively, we can use the expressions for the I -kernels in the weak coupling limit (see eq. (89)) into eq. (91) to evaluate the integrals exactly in the spirit of section III and the answer can be expressed as derivatives. Using these in (74) we can write the total contribution to the interaction energy in the presence of corrugations in the weak limit to be

$$E_{12,W}^{(4)} = \left| E_{\text{Cas},W}^{(0)} \right| \frac{h_1}{a} \frac{h_2}{a} \frac{3}{2} \left[\cos(k_0 y_0) \left(\frac{h_1^2}{a^2} + \frac{h_2^2}{a^2} \right) A_W^{(4)}(k_0 a) - \cos(2k_0 y_0) \frac{1}{2} \frac{h_1}{a} \frac{h_2}{a} A_W^{(4)}(2k_0 a) \right], \quad (96)$$

where in contrast to the result in the Dirichlet limit we observe the appearance of the same function, though with different arguments, as coefficients. This function has been suitably defined as

$$A_W^{(4)}(t_0) = \frac{t_0^5}{4!} \frac{\partial^4}{\partial t_0^4} \left[\frac{1}{t_0} e^{-t_0} \right] = e^{-t_0} \sum_{m=0}^4 \frac{t_0^m}{m!} = \frac{e_4(t_0)}{e^{t_0}}, \quad (97)$$

so that it equals unity at $t_0 = 0$. These are plotted in figure 5. Using eq. (96) in eq. (29) we find that the fourth order contribution to the lateral Casimir force in the weak coupling limit equals

$$F_{\text{Lat},W}^{(4)} = k_0 a \sin(k_0 y_0) \left| F_{\text{Cas},W}^{(0)} \right| \frac{h_1}{a} \frac{h_2}{a} \frac{3}{2} \left[\left(\frac{h_1^2}{a^2} + \frac{h_2^2}{a^2} \right) A_W^{(4)}(k_0 a) - 2 \cos(k_0 y_0) \frac{h_1}{a} \frac{h_2}{a} A_W^{(4)}(2k_0 a) \right]. \quad (98)$$

An exact functional form for the lateral force in the weak coupling limit in the second and fourth order in the perturbative expansion, see eq. (69) and eq. (98), allows us to investigate the approximation involved in the perturbative

analysis more closely. We observe that in each perturbative order the leading powers of $k_0 a$ in the A -function cancels the a dependence in the prefactors associated with h_i . Thus we conclude that the perturbation analysis is valid for $k_0 h \ll 1$. The formal expansions performed in the intermediate steps further restricts our analysis to be valid for $h_1 + h_2 < a$ for arbitrary offset.

V. PROXIMITY FORCE APPROXIMATION

As a preliminary check for the results calculated for the lateral force we shall verify that in the proximity force limit ($k_0 a \rightarrow 0$, keeping h_i/a fixed,) our results in eqs. (63), (69), (95), and (98), reproduce the standard PFA result approximated to appropriate orders in h_i/a . For this purpose let us evaluate the lateral Casimir force in the proximity force approximation for the sinusoidal corrugations described by eq. (56). We begin by writing the distance between the corrugated plates as

$$a(y) = a + h_2 \sin[k_0 y] - h_1 \sin[k_0(y + y_0)]. \quad (99)$$

For sufficiently small a (in comparison to $d = 2\pi k_0^{-1}$) we can treat the plates to be built out of small sections of length dy for which the energy is approximately that of the parallel plate geometry.

1. Dirichlet limit

Using the expression for the Casimir force between parallel plates in the Dirichlet limit we can thus write

$$dE_D^{\text{PFA}}(a(y)) = -L_x dy \frac{\pi^2}{1440} \frac{1}{a(y)^3}, \quad (100)$$

where we interpret $L_x dy$ to be the area of the small section under consideration. Thus the total Casimir energy in this approximation, after interpreting $L_y = \lim_{N \rightarrow \infty} Nd$, will be

$$\begin{aligned} \frac{E_D^{\text{PFA}}}{L_x L_y} &= -\frac{\pi^2}{1440} \frac{1}{a^3} \frac{1}{2\pi} \int_{-\pi}^{\pi} d\theta \frac{1}{\left[1 + \frac{h_2}{a} \sin \theta - \frac{h_1}{a} \sin(\theta + k_0 y_0)\right]^3} \\ &= -\frac{\pi^2}{1440} \frac{1}{a^3} \frac{1}{2\pi} \int_{-\pi}^{\pi} d\theta \frac{1}{\left[1 - \frac{r}{a} \cos \theta\right]^3}, \end{aligned} \quad (101)$$

where we have used the substitutions: $r \sin \alpha = h_2 - h_1 \cos k_0 y_0$, $r \cos \alpha = h_1 \sin k_0 y_0$, and used the periodicity property of the function to eliminate α . We note that $r^2 = h_1^2 + h_2^2 - 2h_1 h_2 \cos(k_0 y_0)$.

As was emphasized in the calculations in the earlier sections we have been subtracting the energies that do not contribute to the torque (or the lateral force) by treating it as a background. This has not been achieved in the above expression in eq. (101) and thus should not be naively compared with our earlier results. But, evaluation of the lateral force will let us compare the expressions. Thus, we calculate the lateral Casimir force in the proximity force approximation, using eq. (101) in eq. (29), to be

$$F_{\text{Lat,D}}^{\text{PFA}} = 2 k_0 a \sin(k_0 y_0) \left| F_{\text{Cas,D}}^{(0)} \right| \frac{h_1}{a} \frac{h_2}{a} \frac{1}{4} \left[\frac{5}{\left(1 - \frac{r^2}{a^2}\right)^{\frac{7}{2}}} - \frac{1}{\left(1 - \frac{r^2}{a^2}\right)^{\frac{5}{2}}} \right], \quad \text{for } |h_1| + |h_2| < a. \quad (102)$$

The basic integral involved in evaluating the above expression is

$$\frac{1}{2\pi} \int_{-\pi}^{\pi} d\theta \frac{1}{(a - r \cos \theta)} = \frac{1}{\sqrt{a^2 - r^2}}, \quad \text{for } r < a, \quad (103)$$

which, after the substitution $z = \exp(i\theta)$, leads to a contour integral on the unit circle in the complex plane. Thus, using Cauchy's theorem only those roots of the denominator that are within the unit circle contribute to the integral.

The PFA result in the leading order for the perturbation parameter is obtained by setting $r = 0$ in eq. (102). This matches exactly with eq. (63) to the leading order in $k_0 a$. This verifies the proximity force limit of the leading order perturbative result. The proximity force limit of the next-to-leading-order result in eq. (95) is similarly verified by matching it with eq. (102) after evaluating eq. (102) to the fourth order in the perturbation parameter.

2. Weak coupling limit

In the weak coupling limit and in the proximity approximation the equation corresponding to eq. (100) is

$$dE_W^{\text{PFA}}(a(y)) = -L_x dy \frac{\lambda_1 \lambda_2}{32 \pi^2} \frac{1}{a(y)} \quad (104)$$

and leads to, after extracting L_y , and proceeding in the same manner as in eq. (101),

$$\frac{E_W^{\text{PFA}}}{L_x L_y} = -\frac{\lambda_1 \lambda_2}{32 \pi^2} \frac{1}{a} \frac{1}{2\pi} \int_{-\pi}^{\pi} d\theta \frac{1}{(1 + \frac{r}{a} \cos \theta)} = -\frac{\lambda_1 \lambda_2}{32 \pi^2} \frac{1}{a} \frac{1}{(1 - \frac{r^2}{a^2})^{\frac{1}{2}}}, \quad \text{for } |h_1| + |h_2| < a. \quad (105)$$

We calculate the lateral Casimir force in the weak coupling limit in the proximity force approximation, using eq. (29), to be

$$F_{\text{Lat,W}}^{\text{PFA}} = k_0 a \sin(k_0 y_0) \left| F_{\text{Cas,W}}^{(0)} \right| \frac{h_1}{a} \frac{h_2}{a} \frac{1}{(1 - \frac{r^2}{a^2})^{\frac{3}{2}}}, \quad \text{for } |h_1| + |h_2| < a. \quad (106)$$

The proximity force limit of the leading- and next-to-leading-order results in the weak coupling limit, eq. (69) and eq. (98), can be verified by keeping the appropriate terms in eq. (106).

VI. ANALYSIS AND DISCUSSION

In this section we shall exclusively deal either in the Dirichlet limit or in the weak coupling limit. We shall further confine ourselves to the case $h_1 = h_2 = h$. Also, we shall find it convenient to define the following dimensionless quantities

$$\mathcal{F}_D \left(k_0 a, \frac{h}{a}, k_0 y_0 \right) = \frac{F_{\text{Lat,D}}(k_0 a, \frac{h}{a}, k_0 y_0)}{2 \left| F_{\text{Cas,D}}^{(0)} \right| \frac{h^2}{a^2} k_0 a \sin(k_0 y_0)}, \quad (107a)$$

$$\mathcal{F}_W \left(k_0 a, \frac{h}{a}, k_0 y_0 \right) = \frac{F_{\text{Lat,W}}(k_0 a, \frac{h}{a}, k_0 y_0)}{\left| F_{\text{Cas,W}}^{(0)} \right| \frac{h^2}{a^2} k_0 a \sin(k_0 y_0)}. \quad (107b)$$

We shall use superscripts $[m, n]$ on these dimensionless quantities to denote the order in the power series expansion to which the lateral force (not \mathcal{F}) have been calculated. In particular m will signify the order in the parameter $k_0 a$, and n will denote the order in h/a . The result in the proximity force approximation should be valid to the first order in $k_0 a$. Thus $\mathcal{F}^{[1, \infty]}$ will represent the PFA result in our notation. The perturbative results are complete in the $k_0 a$ dependence and thus will be denoted by $\mathcal{F}^{[\infty, n]}$. We use square brackets to avoid the confusion it might lead to with the already introduced notation to denote the powers in h_i 's in the superscripts of the A -functions. In these notations our results can be summarized as, (see eqs. (63), (69), (95), (98), (102), and (106),)

$$\mathcal{F}_D^{[\infty, 4]} = A_D^{(1,1)}(k_0 a) + \frac{15}{2} \frac{h^2}{a^2} \left[A_D^{(3,1)}(k_0 a) - \cos(k_0 y_0) A_D^{(2,2)}(k_0 a) \right], \quad \mathcal{F}_D^{[1, \infty]} = \frac{1}{4} \left[\frac{5}{(1 - \frac{r^2}{a^2})^{\frac{7}{2}}} - \frac{1}{(1 - \frac{r^2}{a^2})^{\frac{5}{2}}} \right], \quad (108a)$$

$$\mathcal{F}_W^{[\infty, 4]} = \frac{e_2(k_0 a)}{e^{k_0 a}} + 3 \frac{h^2}{a^2} \left[\frac{e_4(k_0 a)}{e^{k_0 a}} - \cos(k_0 y_0) \frac{e_4(2k_0 a)}{e^{2k_0 a}} \right], \quad \mathcal{F}_W^{[1, \infty]} = \frac{1}{(1 - \frac{r^2}{a^2})^{\frac{3}{2}}}, \quad (108b)$$

where we recall the definition of r after eq. (101). As we mentioned earlier these expressions match to the order $[1, 4]$ both in the Dirichlet and weak limit. Recall, as justified after eq. (98), that $k_0 h$ is the perturbative parameter. Thus, we shall find it convenient to keep $k_0 h$ fixed while discussing the perturbative results. This should be contrasted with the case of proximity force approximation where it is more convenient to keep the parameter h/a fixed. All of the results in eq. (108) are valid for $2h < a$.

1. Dirichlet limit

We plot the lateral force for the Dirichlet limit, $\mathcal{F}_D^{[\infty, 4]}$, with the fractional corrections due to the next-to-leading contribution, in figure 6. The plots diverge as $k_0 a \rightarrow 2k_0 h$ because the perturbation series breaks down beyond that

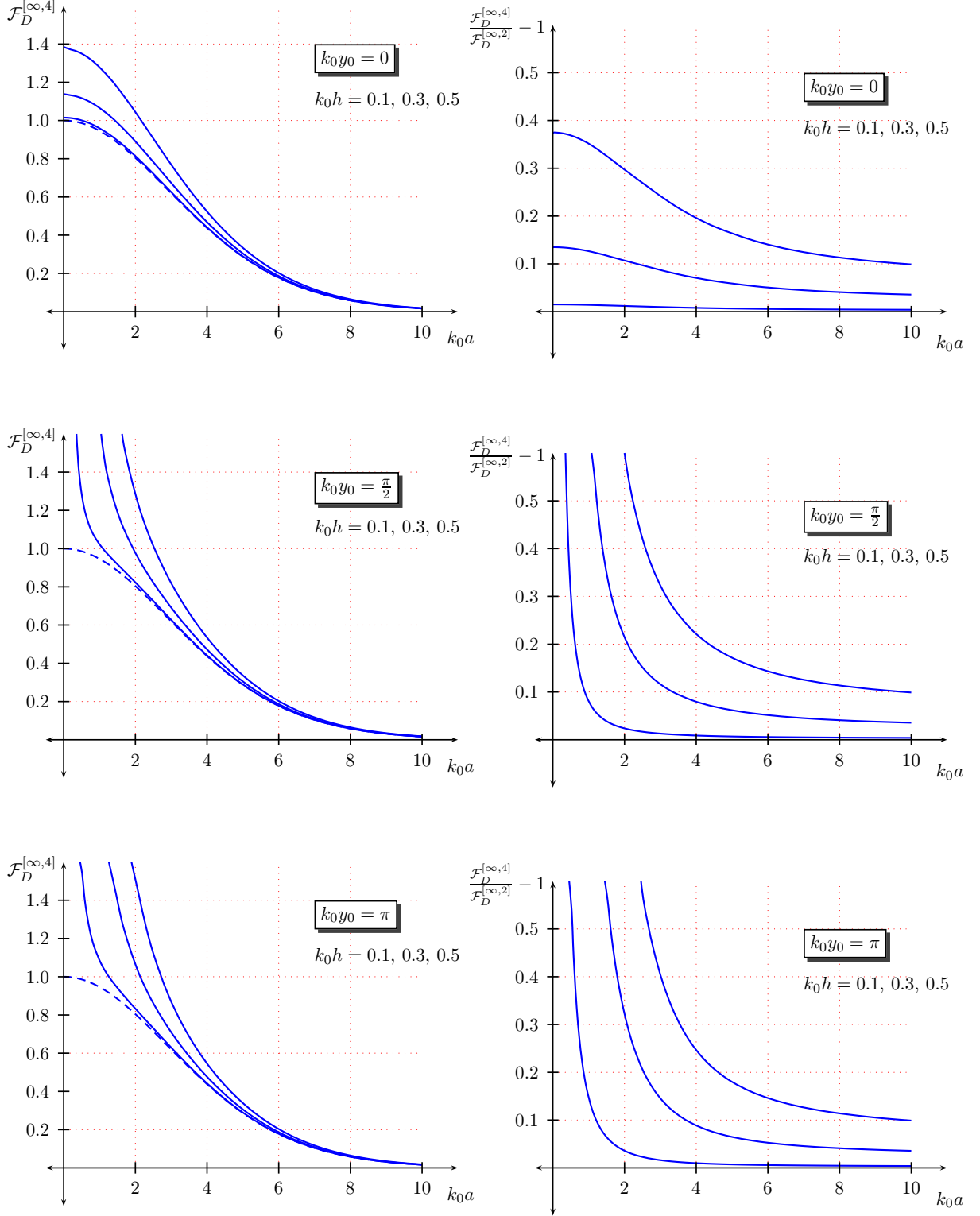


FIG. 6: Dirichlet limit: The plots on the left show $\mathcal{F}_D^{[\infty,4]}$ versus $k_0 a$ for various values of $k_0 y_0$. The dashed curve represents $\mathcal{F}_D^{[\infty,2]}$ which is plotted here for reference. In each plot the higher values of $k_0 h$ deviate more from the reference. The plots on the right show the fractional correction in the next-to-leading order contribution. In each plot the higher values of $k_0 h$ have larger corrections.

point. The plots for $k_0 y_0 = 0$ do not diverge, see eq. (108). We observe that, while keeping $k_0 y_0$ fixed, the fractional corrections due to the next-to-leading order are small for $k_0 h \ll 1$.

In the absence of an exact answer, for the Dirichlet case, to compare with it is not possible to extract the precise error in the perturbative results. In the next section we shall evaluate the corresponding result in the weak coupling limit and evaluate the lateral Casimir force non-perturbatively. We show that the error in the lateral force, for the weak coupling limit, after the next-to-leading order has been included is small for $k_0 h \ll 1$. Presuming that the same would hold for the Dirichlet case, we can expect the error to be sufficiently small for comparison with experimental data. (Comparison with experiments requires the corresponding evaluation for the electromagnetic case, which will be taken up in a later publication.)

2. Weak coupling limit - Non-perturbative results

The plots for the lateral force in the weak coupling limit, $\mathcal{F}_W^{[\infty,4]}$, which have not been displayed here, have the same qualitative content as the Dirichlet case shown in figure 6. To estimate the error in the perturbative results we shall now attempt a non-perturbative evaluation of the lateral Casimir force in the weak coupling limit.

We begin by pointing out the remarkable observation in [17] that exact results for the Casimir force, in the weak coupling limit, can be achieved for specific geometries. This is being extended for a class of geometries, for the scalar case, in [19], and another paper will cover dielectrics in electromagnetism, in [20]. Starting from the central formula in [19], (alternatively using eq. (38), for the weak coupling limit,) we will have

$$\frac{E_W}{L_x} = -\frac{\lambda_1 \lambda_2}{32\pi^3} \int_{-\infty}^{\infty} dy \int_{-\infty}^{\infty} dy' \frac{1}{(y-y')^2 + a(y, y')^2}, \quad (109)$$

where $a(y, y') = a + h_2 \sin[k_0 y'] - h_1 \sin[k_0(y + y_0)]$. Changing variables, $y - y' \rightarrow y$, $y + y' \rightarrow 2\theta/k_0$, and making substitutions very similar to those made after eq. (101), we have

$$\frac{E_W}{L_x L_y} = -\frac{\lambda_1 \lambda_2}{32\pi^2} \frac{1}{2\pi^2} \int_{-\infty}^{\infty} dy \int_0^{2\pi} d\theta \frac{1}{y^2 + [a - r(k_0 y) \cos \theta]^2}, \quad (110)$$

where $r(k_0 y)^2 = h_1^2 + h_2^2 - 2h_1 h_2 \cos(k_0 y + k_0 y_0)$, which is different from the expression for r in the PFA case, presented after eq. (101), in the dependence in the argument of the cosine function. Nevertheless, the θ integral can still be performed using eq. (103) to yield

$$\frac{E_W}{L_x L_y} = -\frac{\lambda_1 \lambda_2}{32\pi^2} \frac{1}{\pi} \int_{-\infty}^{\infty} \frac{dy}{y} \operatorname{Re} \left[\frac{1}{(y + ia)^2 + r(k_0 y)^2} \right]^{\frac{1}{2}}, \quad \text{for } |h_1| + |h_2| < a. \quad (111)$$

Using the above expression in eq. (29) we calculate the lateral force per unit area in the weak coupling limit to be

$$\frac{F_{\text{Lat},W}}{L_x L_y} = -\frac{\lambda_1 \lambda_2}{32\pi^2} \frac{h_1}{a^2} \frac{h_2}{a} (k_0 a)^4 \frac{1}{\pi} \int_{-\infty}^{\infty} \frac{dt}{t} \operatorname{Re} \left[\frac{\sin(t + k_0 y_0)}{[(t + ik_0 a)^2 + \{k_0 r(t)\}^2]^{\frac{3}{2}}} \right], \quad \text{for } |h_1| + |h_2| < a. \quad (112)$$

Expanding the denominator in the above expression as a power series in $k_0 r/(t + ik_0 a)$, lets us evaluate the integral using the residue theorem. We can thus write, after letting $h_1 = h_2 = h$, which leads to the simplification, $r(k_0 y_0) = 2h \sin[(k_0 y + k_0 y_0)/2]$,

$$\frac{F_{\text{Lat},W}}{L_x L_y} = \frac{\lambda_1 \lambda_2}{32\pi^2 a^2} (k_0 a)^2 \operatorname{Re} \left[\frac{e^{-ik_0 y_0}}{(-i)} \sum_{n=0}^{\infty} \frac{1}{[n!]^2} \frac{1}{2n+2} \left(h \frac{\partial}{\partial a} \right)^{2n+2} \frac{1}{k_0 a} e^{-k_0 a} \sin^{2n} \left(\frac{k_0 y_0}{2} - i \frac{k_0 a}{2} \right) \right], \quad (113)$$

which reproduces the leading and next-to-leading results in eqs. (69) and (98) for the case $n = 0$ and $n = 1$ respectively. This structure justifies our presumption that the perturbative analysis holds as an asymptotic expansion as $k_0 h \rightarrow 0$. Expressing the above sum in a closed form, or evaluation of the integral in eq. (112), would lead to an exact expression for the lateral force in the weak coupling limit. We have not been able to achieve either, however, so we shall rely on numerical evaluation.

In terms of the notation introduced in eq. (107) we can write eq. (112) as

$$\mathcal{F}_W^{[\infty,\infty]} = -\frac{(k_0 a)^3}{\sin(k_0 y_0)} \frac{1}{\pi} \int_{-\infty}^{\infty} \frac{dt}{t} \operatorname{Re} \left[\frac{\sin(t + k_0 y_0)}{[(t + ik_0 a)^2 + \{k_0 r(t)\}^2]^{\frac{3}{2}}} \right], \quad \text{for } 2h < a. \quad (114)$$

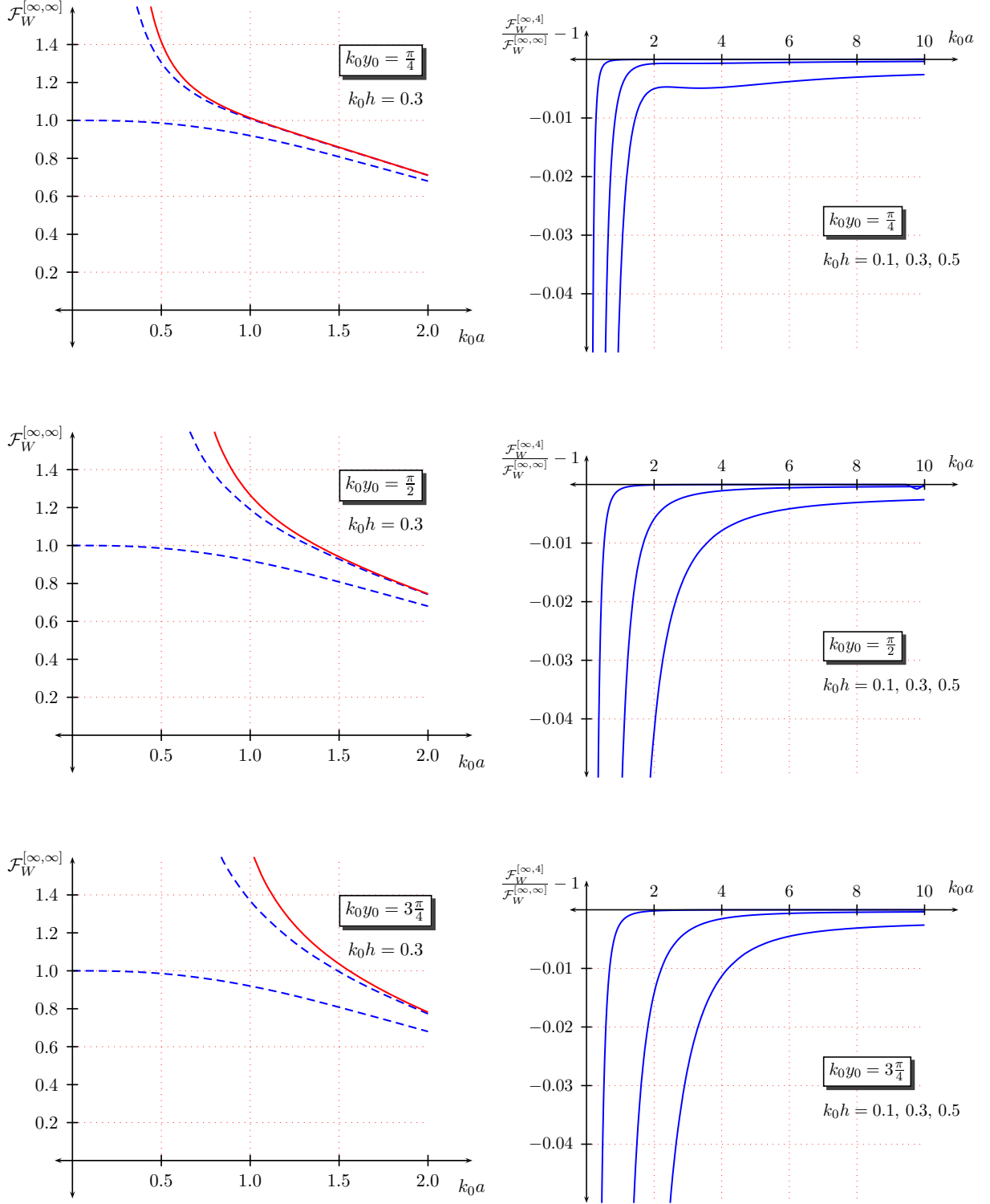


FIG. 7: Weak coupling limit: The plots on the left show $\mathcal{F}_D^{[\infty, \infty]}$ versus $k_0 a$ for various values of $k_0 y_0$ at $k_0 h = 0.3$. The dashed curves represents $\mathcal{F}_D^{[\infty, 2]}$ and $\mathcal{F}_D^{[\infty, 4]}$ which is plotted here for reference. In each plot the exact value is greater than the value estimated by $\mathcal{F}_D^{[\infty, 4]}$. The plots on the right show the fractional error in the perturbative result. In each plot the higher values of $k_0 h$ have larger errors.

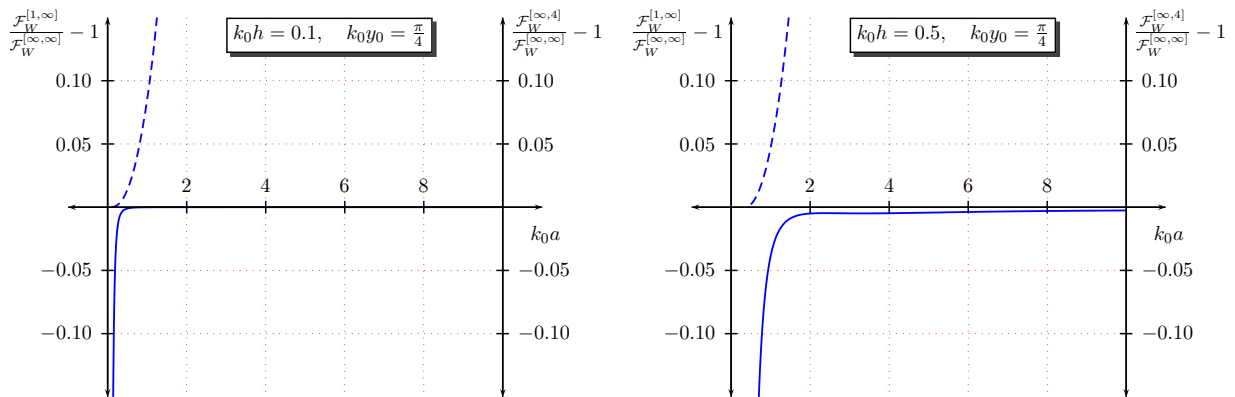


FIG. 8: Weak coupling limit: Fractional error in PFA is plotted as the dashed curve. The corresponding error in the perturbative result is plotted as the bold curve and is described by the axis on the right.

The above non-perturbative expression for the lateral Casimir force on corrugated plates, in the weak coupling limit, has been plotted in figure 7. For comparison purposes the perturbative results are plotted as dashed curves in figure 7. Actually, we found the numerical evaluation of eq. (110), after evaluating the derivative with respect to y_0 , easier than that of eq. (114). We observe that the perturbative results, when the next-to-leading order is included, compares with the exact result remarkably well for $k_0 h \ll 1$ and $2h < a$. The fractional error in the lateral force when the next-to-leading order contribution is included is displayed on the right column in figure 7.

3. Validity of PFA

We shall now compare the PFA result in the weak limit, derived in eq. (106), with the non-perturbative result in eq. (112). In figure 8 we plot the fractional error in the PFA result, for fixed $k_0 h$, and compare it to the fractional error in the perturbative results. We note that PFA is a good approximation for $k_0 a \ll 1$ and perturbative results are valid for $k_0 h \ll 1$. Both the PFA and the perturbative analysis are restricted to $2h < a$. The $2h < a$ restriction is necessary for the force being finite, due to non-overlapping of the potentials for arbitrary offset. For special offsets, the restriction is weaker, and there is no restriction at all, for zero offset. The precise dependence of the restriction on the offset is gotten by referring to eq. (106) and observing that the validity regime is $r = 2h \sin(k_0 y_0/2) < a$.

A recent debate, see [11, 12, 13], involved the comparison of the PFA result and the perturbative result. We earlier noted that the PFA limit is obtained by taking the limit $k_0 a \rightarrow 0$ while keeping the ratio h/a fixed. In figure 9 we plot the lateral force in the PFA limit and compare it with the non-perturbative result for various values of $k_0 a$. This justifies our presumption that the PFA is a good approximation for $k_0 a \ll 1$. We note that the error in the PFA is less than 1% for $k_0 a \ll 1$ for arbitrary h/a . For $k_0 y_0 = \pi/4$, we observe that the PFA is a very good approximation for $h \sim a$ which satisfies $2h \sin(k_0 y_0/2) < a$. After viewing the plots for various values of $k_0 y_0$ we note that in general the PFA is a good approximation for $h \sim a$ and further beyond for offsets $k_0 y_0 < \pi/4$. It is, in fact, plausible that the PFA holds for large amplitude corrugations for small offsets because the corrugations fit together like fingers in a glove.

Acknowledgments

We thank Jef Wagner for extensive collaborative assistance throughout this project. KVS would like to thank Osama Alkhouli, Subrata Bal, Pravin Chaubey, James Dizikes, David Hartnett, K. V. Jupesh, Sai Krishna Rao, S. Shankar, and Stéphane Valladier, for discussions, comments, and help with programming in Mathematica. We thank Steve Fulling for constructive comments on the manuscript. We thank the US National Science Foundation (Grant No. PHY-0554926) and the US Department of Energy (Grant No. DE-FG02-04ER41305) for partially funding this research. ICP would like to thank the French National Research Agency (ANR) for support through Carnot funding.

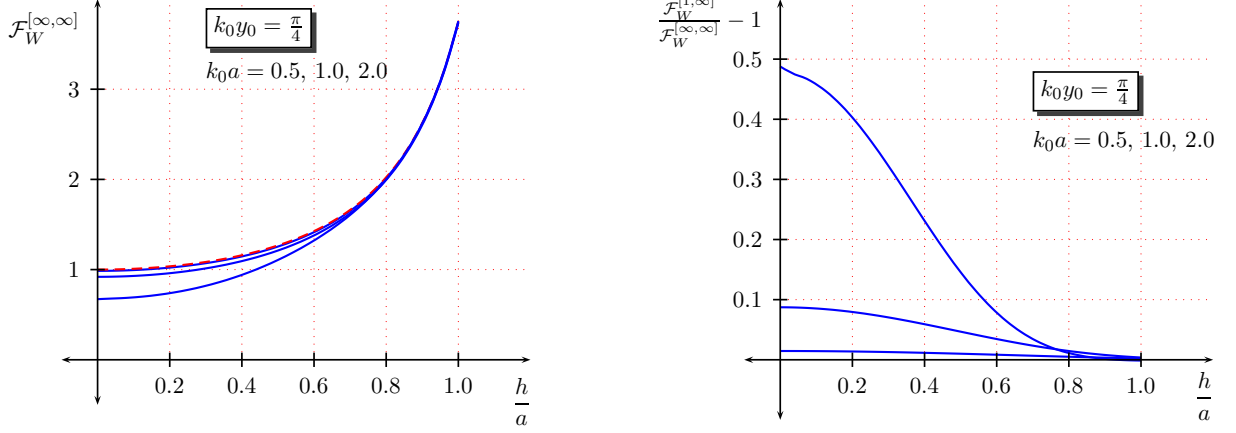


FIG. 9: Weak coupling limit: On the left the PFA is shown as the dashed curve. The exact results for higher values of $k_0 a$ are seen to deviate from the dashed curve. On the right the fractional error in PFA is shown to increase with higher values of $k_0 a$.

APPENDIX A: DERIVATIVES OF THE GREEN'S FUNCTION

Evaluation of eq. (47) involves taking derivatives of the Green's function which as we shall see involves evaluating a function at a point where it has jump discontinuities in the derivatives. We start by noting that the differential equation in eq. (43) can be solved in terms of exponential functions in the different regions described in figure 10. Explicitly the solutions are given by the following piecewise-defined functions, with subscripts denoting the regions they are defined in,

$$g_1^{(0)}(z, z'; \kappa) = \frac{1}{2\kappa} e^{-\kappa|z-z'|} - \frac{1}{\Delta} \frac{1}{2\kappa} e^{\kappa(z+z')} \left[\frac{\lambda_1}{2\kappa} e^{-2\kappa a_1} + \frac{\lambda_2}{2\kappa} e^{-2\kappa a_2} - \frac{\lambda_1 \lambda_2}{2\kappa} \left(e^{-2\kappa a_2} - e^{-2\kappa a_1} \right) \right], \quad (\text{A1a})$$

$$g_2^{(0)}(z, z'; \kappa) = \frac{1}{2\kappa} e^{-\kappa|z-z'|} - \frac{1}{\Delta} \frac{1}{2\kappa} \left[\frac{\lambda_2}{2\kappa} \left(1 + \frac{\lambda_1}{2\kappa} \right) e^{\kappa(z+z'-2a_2)} + \frac{\lambda_1}{2\kappa} \left(1 + \frac{\lambda_2}{2\kappa} \right) e^{-\kappa(z+z'-2a_1)} - \frac{\lambda_1 \lambda_2}{2\kappa} e^{\kappa(z-z'-2a)} - \frac{\lambda_1 \lambda_2}{2\kappa} e^{-\kappa(z-z'+2a)} \right], \quad (\text{A1b})$$

$$g_3^{(0)}(z, z'; \kappa) = \frac{1}{2\kappa} e^{-\kappa|z-z'|} - \frac{1}{\Delta} \frac{1}{2\kappa} e^{-\kappa(z+z')} \left[\frac{\lambda_1}{2\kappa} e^{2\kappa a_1} + \frac{\lambda_2}{2\kappa} e^{2\kappa a_2} - \frac{\lambda_1 \lambda_2}{2\kappa} \left(e^{2\kappa a_1} - e^{2\kappa a_2} \right) \right], \quad (\text{A1c})$$

$$g_4^{(0)}(z, z'; \kappa) = \frac{1}{\Delta} \frac{1}{2\kappa} \left[\left(1 + \frac{\lambda_2}{2\kappa} \right) e^{\kappa(z-z')} - \frac{\lambda_2}{2\kappa} e^{\kappa(z+z'-2a_2)} \right], \quad (\text{A1d})$$

$$g_5^{(0)}(z, z'; \kappa) = \frac{1}{\Delta} \frac{1}{2\kappa} e^{\kappa(z-z')}, \quad (\text{A1e})$$

$$g_7^{(0)}(z, z'; \kappa) = \frac{1}{\Delta} \frac{1}{2\kappa} \left[\left(1 + \frac{\lambda_1}{2\kappa} \right) e^{\kappa(z-z')} - \frac{\lambda_1}{2\kappa} e^{-\kappa(z+z'-2a_1)} \right], \quad (\text{A1f})$$

where

$$\Delta = 1 + \frac{\lambda_1}{2\kappa} + \frac{\lambda_2}{2\kappa} + \frac{\lambda_1 \lambda_2}{2\kappa} \left(1 - e^{-2\kappa a} \right). \quad (\text{A2})$$

Using the reciprocal symmetry of the Green's function we further have $g_6^{(0)}(z, z'; \kappa) = g_4^{(0)}(z', z; \kappa)$, $g_8^{(0)}(z, z'; \kappa) = g_5^{(0)}(z', z; \kappa)$, and $g_9^{(0)}(z, z'; \kappa) = g_7^{(0)}(z', z; \kappa)$. The above piecewise solution gives the complete Green's function.

It is of relevance to observe that the Green's function represented above is continuous everywhere in the z, z' domain while its first derivatives have simple (jump) discontinuities along the lines, $z = z'$, $z = a_{1,2}$, and $z' = a_{1,2}$. Since the evaluation of I -kernels in eq. (47), and in eq. (80), involves taking derivatives of the Green's function at the lines of discontinuity, a definite prescription for the evaluation of the derivatives is called for. For this purpose, we interpret the value of a function at the point where it has a jump discontinuity to be the average of all the possible limiting

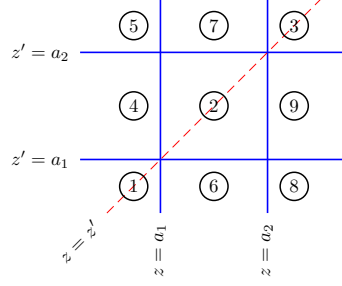


FIG. 10: Description of the regions in the $z - z'$ domain on which the piecewise functions contributing to the Green's function are defined.

values. For example, the derivative of the Green's function at the point $(z = a_2, z' = a_1)$ in figure 10 takes on four different values when approached from the four regions 2, 6, 8, and 9. The value of the derivative is defined as the average of these four values.

We provide the following supporting arguments for the averaging prescription. Firstly, we note that eq. (47) was derived from eq (41) after integrating over the complete $z - z'$ domain. The potentials in eq (41) involved derivatives of delta functions, and after integration by parts the integrals got contributions from a single point in the $z - z'$ domain. Since an integral is a sum we expect it to support the averaging prescription. The second justification we provide is in the way of verification for known examples. We made checks by using this prescription to analyze the Green's function for the case of a single plate. We do not provide the details of the exercise here.

Evaluation of the derivatives using the averaging prescription is made convenient when we define the Green's function around a point as the average of the suitable piecewise functions. Thus, we evaluate

$$\begin{aligned}
 g^{(0)}(a_1, a_2; \kappa) &= \frac{1}{4} \left[g_2^{(0)}(a_1, a_2; \kappa) + g_4^{(0)}(a_1, a_2; \kappa) + g_5^{(0)}(a_1, a_2; \kappa) + g_7^{(0)}(a_1, a_2; \kappa) \right] = \frac{1}{\Delta} \frac{1}{2\kappa} e^{-\kappa a}, \\
 g^{(0)}(a_2, a_1; \kappa) &= \frac{1}{4} \left[g_2^{(0)}(a_2, a_1; \kappa) + g_6^{(0)}(a_2, a_1; \kappa) + g_8^{(0)}(a_2, a_1; \kappa) + g_9^{(0)}(a_2, a_1; \kappa) \right] = \frac{1}{\Delta} \frac{1}{2\kappa} e^{-\kappa a}, \\
 g^{(0)}(a_1, a_1; \kappa) &= \frac{1}{4} \left[g_1^{(0)}(a_1, a_1; \kappa) + g_2^{(0)}(a_1, a_1; \kappa) + g_4^{(0)}(a_1, a_1; \kappa) + g_6^{(0)}(a_1, a_1; \kappa) \right] = \frac{1}{\Delta} \frac{1}{2\kappa} \left[1 + \frac{\lambda_2}{2\kappa} (1 - e^{-2\kappa a}) \right], \\
 g^{(0)}(a_2, a_2; \kappa) &= \frac{1}{4} \left[g_2^{(0)}(a_2, a_2; \kappa) + g_3^{(0)}(a_2, a_2; \kappa) + g_7^{(0)}(a_2, a_2; \kappa) + g_9^{(0)}(a_2, a_2; \kappa) \right] = \frac{1}{\Delta} \frac{1}{2\kappa} \left[1 + \frac{\lambda_1}{2\kappa} (1 - e^{-2\kappa a}) \right].
 \end{aligned}$$

The first derivatives evaluate to be

$$\partial_z g^{(0)}(z, z'; \kappa) \Big|_{z=a_1, z'=a_2} = \frac{1}{\Delta} \frac{\kappa}{2\kappa} \left(1 + \frac{\lambda_1}{2\kappa} \right) e^{-\kappa a}, \quad (\text{A4a})$$

$$\partial_{z'} g^{(0)}(z, z'; \kappa) \Big|_{z=a_1, z'=a_2} = -\frac{1}{\Delta} \frac{\kappa}{2\kappa} \left(1 + \frac{\lambda_2}{2\kappa} \right) e^{-\kappa a}, \quad (\text{A4b})$$

$$\partial_z g^{(0)}(z, z'; \kappa) \Big|_{z=a_1, z'=a_1} = -\frac{1}{\Delta} \frac{\kappa}{2\kappa} \frac{\lambda_2}{2\kappa} e^{-\kappa a}, \quad (\text{A4c})$$

$$\partial_z g^{(0)}(z, z'; \kappa) \Big|_{z=a_2, z'=a_2} = \frac{1}{\Delta} \frac{\kappa}{2\kappa} \frac{\lambda_1}{2\kappa} e^{-\kappa a}. \quad (\text{A4d})$$

where $\partial_{z, z'}$ is derivative with respect to z, z' . The second derivatives involving two distinct variables evaluate to be

$$\partial_z \partial_{z'} g^{(0)}(z, z'; \kappa) \Big|_{z=a_1, z'=a_2} = -\frac{1}{\Delta} \frac{\kappa^2}{2\kappa} \left(1 + \frac{\lambda_1}{2\kappa} \right) \left(1 + \frac{\lambda_2}{2\kappa} \right) e^{-\kappa a}, \quad (\text{A5a})$$

$$\partial_z \partial_{z'} g^{(0)}(z, z'; \kappa) \Big|_{z=a_1, z'=a_1} = -\frac{1}{\Delta} \frac{\kappa^2}{2\kappa} \left[\left(1 + \frac{\lambda_1}{2\kappa} \right) \left(1 + \frac{\lambda_2}{2\kappa} \right) + \frac{\lambda_2}{2\kappa} e^{-2\kappa a} \right], \quad (\text{A5b})$$

$$\partial_z \partial_{z'} g^{(0)}(z, z'; \kappa) \Big|_{z=a_2, z'=a_2} = -\frac{1}{\Delta} \frac{\kappa^2}{2\kappa} \left[\left(1 + \frac{\lambda_1}{2\kappa} \right) \left(1 + \frac{\lambda_2}{2\kappa} \right) + \frac{\lambda_1}{2\kappa} e^{-2\kappa a} \right]. \quad (\text{A5c})$$

The second derivatives involving the same variables evaluate to

$$\partial_z^2 g^{(0)}(z, z'; \kappa) = \kappa^2 g^{(0)}(z, z'; \kappa) \quad (\text{A6})$$

which when compared with eq. (43) tells us that the averaging prescription practically throws away the delta function contributions in eq. (43). A more detailed study of this issue is being sought. Since the second derivative returns the Green's function back, all higher order derivatives are obtained in terms of the above expressions.

APPENDIX B: COMPARISON OF OUR LEADING ORDER RESULT WITH REFERENCE [6]

Here we wish to explicitly compare our results—in the leading order—with those in [6]. In particular we show how the Dirichlet limit of our expression for the interaction energy in the leading order [eq. (44) with eq. (51) inserted] matches with the results in [6] [eq. (11) with eqs. (13) and (17) there]. To this end we begin from eq. (41) and write the interaction energy in the form

$$E_{12}^{(2)} = - \int d(t-t') \int \int dx dy \int \int dx' dy' h_1(y) Q(|\mathbf{y} - \mathbf{y}'|) h_2(y'), \quad (\text{B1})$$

where we have used the notation introduced in [6]: $\mathbf{y} \equiv (t, x, y)$, $|\mathbf{y} - \mathbf{y}'|^2 = (t-t')^2 + (x-x')^2 + (y-y')^2$, and switched to Euclidean time by replacing $t, t', \tau \rightarrow -it, -it', -i\tau$. The Q -kernel introduced above, following [6], is given as

$$Q(|\mathbf{y} - \mathbf{y}'|) = \frac{\lambda_1 \lambda_2}{2} \frac{\partial}{\partial z} \frac{\partial}{\partial z'} \left[G_E^{(0)}(\mathbf{x}, t, \mathbf{x}', t') G_E^{(0)}(\mathbf{x}', t', \mathbf{x}, t) \right] \Big|_{z'=a_1, z=a_2}, \quad (\text{B2})$$

where $\mathbf{x} \equiv (x, y, z)$ and $G_E^{(0)}(\mathbf{x}, t, \mathbf{x}', t')$ is given in terms of eq. (42) after switching to Euclidean time as

$$G_E^{(0)}(\mathbf{x}, t, \mathbf{x}', t') = \frac{1}{i} G^{(0)}(\mathbf{x}, t, \mathbf{x}', t') = \int \frac{d^3 \kappa}{(2\pi)^3} e^{i\kappa \cdot (\mathbf{y} - \mathbf{y}')} g^{(0)}(z, z'; \kappa), \quad (\text{B3})$$

where $\kappa \equiv (\zeta, k_x, k_y)$ and $\mathbf{y} = (t, x, y)$, $\mathbf{y}' = (t', x', y')$.

Dirichlet Limit

In the Dirichlet limit the above expression should correspond to the Q -kernel introduced in [6] [eq. (13) there]. Note that in [6] the interaction energy is not isolated from the outset unlike in our eq. (37). This is achieved in [6] by identifying and subtracting the contributions to the energy from the single plates. We identify the presence of our I -kernel [see eq. (47)] in eq. (B2) which lets us express the Dirichlet limit of the Q -kernel, using eq. (50), in the form

$$Q_D(|\mathbf{y} - \mathbf{y}'|) = \frac{1}{2} \left[\int \frac{d^3 \kappa}{(2\pi)^3} e^{i\kappa \cdot (\mathbf{y} - \mathbf{y}')} \frac{\kappa}{\sinh \kappa a} \right]^2 = \frac{1}{2} \left[\frac{1}{a^4} P\left(\frac{|\mathbf{y} - \mathbf{y}'|}{a}\right) \right]^2 \quad (\text{B4})$$

in terms of the integral

$$P(x) = \frac{1}{2\pi^2} \frac{1}{x} \int_0^\infty t^2 dt \frac{\sin(tx)}{\sinh t} = \frac{\pi}{8} \frac{1}{x} \frac{\sinh(\pi x/2)}{\cosh^3(\pi x/2)}. \quad (\text{B5})$$

This exact form for the Q -kernel in the Dirichlet limit reproduces the result in [6].

This exact form for the Q -kernel in the Dirichlet limit suggests that we can consider a class of corrugations for which exact results, in the perturbative approximation, might be achievable. Like the exact results achieved in [19, 20] for the weak coupling limit, we should be able to explore geometries in the Dirichlet limit in the perturbative approximation starting from eq. (B1). Further, it should also be possible to extend these explorations to the next-to-leading orders. And, for very special geometries it might just be possible to transcend the perturbative approximation and get exact results in the Dirichlet limit alone. We hope to be able to address some of these explorations in our forthcoming publications.

[1] H. B. G. Casimir, Kon. Ned. Akad. Wetensch. Proc. **51**, 793 (1948).

- [2] Yu. S. Barash, *Izv. Vuzov. Ser. Radiofiz.* **16**, 1086 (1973) [*Sov. Radiophys.* **16**, 945 (1973)].
- [3] R. Golestanian and M. Kardar, *Phys. Rev. Lett.* **78**, 3421 (1997) [arXiv:quant-ph/9701005].
- [4] R. Golestanian and M. Kardar, *Phys. Rev. A* **58**, 1713 (1998).
- [5] T. Emig, A. Hanke, R. Golestanian and M. Kardar, *Phys. Rev. Lett.* **87**, 260402 (2001) [arXiv:cond-mat/0106028].
- [6] T. Emig, A. Hanke, R. Golestanian and M. Kardar, *Phys. Rev. A* **67**, 022114 (2003).
- [7] R. Buscher and T. Emig, *Phys. Rev. A* **69**, 062101 (2004) [arXiv:cond-mat/0401451].
- [8] A. Roy and U. Mohideen, *Phys. Rev. Lett.* **82**, 4380 (1999).
- [9] F. Chen, U. Mohideen, G. L. Klimchitskaya, and V. M. Mostepanenko, *Phys. Rev. Lett.* **88**, 101801 (2002).
- [10] F. Chen, U. Mohideen, G. L. Klimchitskaya, and V. M. Mostepanenko, *Phys. Rev. A* **66**, 032113 (2002).
- [11] R. B. Rodrigues, P. A. Maia Neto, A. Lambrecht, and S. Reynaud, *Phys. Rev. Lett.* **96**, 100402 (2006).
- [12] F. Chen, U. Mohideen, G. L. Klimchitskaya, and V. M. Mostepanenko, *Phys. Rev. Lett.* **98**, 068901 (2007).
- [13] R. B. Rodrigues, P. A. Maia Neto, A. Lambrecht, and S. Reynaud, *Phys. Rev. Lett.* **98**, 068902 (2007).
- [14] I. Cavero-Peláez, K. A. Milton, P. Parashar and K. V. Shajesh, arXiv:0805.2777 [hep-th].
- [15] T. Emig, N. Graham, R. L. Jaffe and M. Kardar, *Phys. Rev. D* **77**, 025005 (2008) [arXiv:0710.3084 [cond-mat.stat-mech]].
- [16] O. Kenneth and I. Klich, *Phys. Rev. Lett.* **97**, 160401 (2006) [arXiv:quant-ph/0601011].
- [17] K. A. Milton and J. Wagner, *J. Phys. A* **41**, 155402 (2008) [arXiv:0712.3811 [hep-th]].
- [18] K. A. Milton, *J. Phys. A* **37**, 6391 (2004) [arXiv:hep-th/0401090].
- [19] K. A. Milton, P. Parashar and J. Wagner, in preparation.
- [20] K. A. Milton, P. Parashar and J. Wagner, arXiv:0806.2880 [hep-th].